*Master Thesis*
*Electrical Engineering*
*June 2013*

# *Enhancement of SAR Image Resolution with Implementation of Circular GB-SAR System*

***Dheeraj Nehru Neravati***

This thesis is presented as part of Degree of
Master of Science in Electrical Engineering with emphasis on Radio Communication

*Blekinge Institute of Technology (BTH)*
*June 2013*

**Blekinge Institute of Technology, Sweden**
**School of Engineering**
**Department of Electrical Engineering**
**Supervisor:** **Dr. Viet Thuy Vu**
**Co-Supervisor:** **Prof. Mats Pettersson**
**Examiner:** **Dr. Benny Lövström**

This thesis is submitted to the School of Engineering at Blekinge Institute of Technology in partial fulfilment of the requirements for the degree of Master of Science in Electrical Engineering with emphasis on Radio Communication.


**Contact Information:**

**Author:**
*Dheeraj Nehru Neravati*
Dept. of Electrical Engineering
School of Engineering
Blekinge Institute of Technology (BTH), Sweden.
E-mail: dhne10@student.bth.se, Dheeraj.N.Neravati@ieee.org

**University Advisor:**
*Dr. Viet Thuy Vu*
Dept. of Electrical Engineering
School of Engineering
Blekinge Institute of Technology (BTH), Sweden.
E-mail: viet.thuy.vu@bth.se

**University Co - Advisor:**
*Prof: Mats Pettersson*
Dept. of Electrical Engineering
School of Engineering
Blekinge Institute of Technology
E-mail: mats.pettersson@bth.se

**Examiner:**
*Dr. Benny Lövström*
Dept. of Electrical Engineering
School of Engineering
Blekinge Institute of Technology (BTH), Sweden.
E-mail: benny.lovstrom@bth.se

# Abstract

Radars were used for surveillance and remote sensing but nowadays they handle a vast range of applications, radar imagery being one of them. The need for high resolution images was inevitable which lead to Synthetic Aperture Radar (SAR) systems. SAR plays a prominent role in remote sensing applications and geophysical studies. SAR is an imaging Radar which inherits advantages over conventional optic sensors since they can be used irrespective of the climatic conditions and sunlight due to the merits of microwaves. In addition to these benefits SAR generates a finer resolution 2-D image which cannot be achieved with conventional real aperture radar. Ground-based SAR has a wide range of applications like monitoring of post land slide surface to estimate slope displacements, observation of Tsunami affected area for ground surface movements, etc...

In the modern times, improvement in the resolution was still anticipated and this requirement for technological advancement forces the researchers to implement new strategies for the enhancement of SAR image resolution in both azimuth and range directions. In this thesis we use the circular aperture technique for resolution enhancement with practical implementation of an experimental model at the laboratory and analyzing the results with those corresponding to linear aperture.

In this thesis we make use of Ultra wideband–Ultra wide beam (UWB) ground based SAR system (GB-SAR) system which achieves better resolution SAR images in both azimuth and range directions. GBP (Global Back Projection) algorithm is used to reconstruct the image from the pulse compressed back scattered echo signal.

This thesis is divided into two parts: the first part concentrates on the establishment and data processing of GB-SAR whereas the second part focuses on the resolution enhancement of SAR images using circular apertures. In the first part experimental GB-SAR system is introduced and the data processing with radar signal reconstruction and image processing technique is explained in detail. The SAR image formed by the experimental data is examined and compared with the assessments in theory. In the second part an experiment with circular aperture i.e. GB-CSAR system is performed to obtain the enhancement of image resolution. The SAR image formed with the experimental CSAR data is compared with the experimental LSAR image and resolution is investigated.

Thus analysis on efficiency of radar resolution between Linear SAR and Circular SAR is established with practical implementation of SAR system at the laboratory. Results emphasize the significance of Circular SAR over Liner SAR.

# Preface

This master thesis summarizes my work in the field of synthetic aperture radar. This work has been performed at department of electrical engineering at Blekinge Institute of Technology.

This thesis consists of six chapters followed by two scientific papers and a technical report:

- Viet T. Vu, Dheeraj N. Nehru, Thomas K. Sjögren and Mats I. Pettersson, “An experimental ground-based SAR system for studying SAR fundamentals”, in *Proc. APSAR 2013*, Tsukuba, Japan, Sep. 2013, pp. 1–4.

- Dheeraj N. Nehru, Viet T. Vu, Thomas K. Sjögren and Mats I. Pettersson, “SAR resolution enhancement with circular aperture in theory and empirical scenario”, *submitted to IEEE RadarCon 2014*, Cincinnati, USA, May 2014.

- Dheeraj N. Nehru, “Technical report on GB-SAR experiments”, in *BTH Research Articles*, June 2013.

# Acknowledgements

This work wouldn't have been possible without the support and encouragement of people around me. I would like to express my thankfulness for them.

I would like to give a sincere thanks to my parents and my sister who have always been supporting me in all parts of my life for which my mere expression of thanks won't be sufficient. I am grateful for their encouragement and everlasting love and support.

I would like to express my deepest gratitude to my supervisor *Dr. Viet Thuy Vu* whose encouragement helped me a lot to finish this work in an effective manner. I was very fortunate to get him as an advisor who helped me to increase my knowledge about SAR processing concepts. His expertise guidance, advises and valuable discussions made me acquire good knowledge in SAR. His continuous availability and friendly nature was very supporting.

I would also like to express my deepest gratitude to my co-supervisor *Prof. Mats I. Pettersson* who created interest in me on antennas & SAR with his expertise teaching and guidance during my antenna course. I am very thankful for his encouragement and guidance during my thesis.

I would like to thank *Dr. Thomas Sjörgen* for his questions and discussions which were very helpful.

I would like to thank my examiner *Dr. Benny Lövström* for his encouragement.

*Dheeraj Nehru Neravati*
Karlskrona, Sweden
June 2013

## Table of Contents

# List of Figures & Tables:

“This work is dedicated to my mom Rama Devi and dad Prasad”.

# Chapter 1

# Motivation and Background

Radars are crucial microwave devices with wide range of applications in the modern times. Synthetic Aperture Radars are kind of imaging radars with high resolution capability. SAR takes a wide range of applications in military sector as well as in civilian purposes such as: for vegetation analysis (ref. national park in India) [1], understand the plant evaluation, soil moisture analysis [2], analysis of animal and human habitat [3], behind the wall identification i.e see through the wall application (STTW) [4], mines detection in military applications [5], maritime applications such as aqua culture, oceanic analysis, oil spill detection and analysis [6], oil thickness detection, monitoring of oil wells, monitoring of hill slides and landslides[7], monitoring of a monument[8], space exploration, monitoring of polar ice caps, remote sensing [9], recently research was carried out to investigate the applications of SAR in meteorology for climate analysis [10], etc...

With such wide range of applications and with growing requirements and functions, need for improvement of resolution is further anticipated. Need of higher resolution is due to the features it exhibits, for example elements in the image of the ground (taken by an imaging SAR system) can be clearly observed and distinguished, during the analysis of animal and human habitat or during vegetation analysis higher resolutions helps in improving the accuracies. During monitoring of monument or monitoring of hill slides and landslides higher resolutions are required for effective measurements. Consider a vehicle missing in the forest or a small glider plane crashed in the forest, in such case our requirement of detecting the objects can’t be effective unless and until images of satisfactory resolution are available. Commonly and most importantly enhancement of resolution help to fetch out more and accurate information from the image scene in any kind of application. This requirement for the advancement of technology forces the developers to implement novel strategies for the

enhancement of resolution. This need for enhancement of resolution instigated me and was instrumental for the initiation of this thesis.

Extreme integration angles and wide beam antennas can be used for the purpose of resolution improvement in azimuth direction and wide band pulses can be used for resolution improvement in range direction. In this thesis circular aperture was used which has the integration angle of $360^0$ and made use of Ultra wide band – Ultra wide beam horn antenna which gives better resolution in both range and azimuth directions. Experimental ground based circular SAR system was developed in the laboratory according to the suitable parameters and constraints

This thesis is divided into two parts:

The first part concentrates on the establishment and data processing of ground based SAR system (GB-SAR) whereas the second part focuses on the resolution enhancement of SAR images using circular apertures. In the first part experimental GB-SAR system is introduced and the data processing with radar signal reconstruction and image processing technique is explained in detail. The SAR image formed by the experimental data is examined and compared with the assessments in theory.

In the second part the experimental data of circular aperture i.e. GB-CSAR system is used to verify the enhancement of image resolution. The SAR image formed with the experimental CSAR data is compared with the experimental LSAR image and resolution is investigated.

The aim of this thesis is to find a strategy to enhance the resolution of a SAR image. Thus we make an experimental model and explore the advantages of circular apertures. Results obtained are compared with its linear aperture counterparts.

**Outline of the thesis:-**

Thesis consists of five chapters and two papers organised in the following way.

- Chapter 2 consists of the main concepts of radar and Synthetic Aperture Radar (SAR) fundamentals.
- Chapter 3 describes the SAR signal processing algorithms.
- Chapter 4 discusses the Ground-Based SAR system.
- Chapter 5 focuses on the thesis overview and the two papers.

# Chapter 2

# Radar and SAR Fundamentals

## 2.1 Radar

Radar stands for Radio detection and ranging. As the name suggests it is a device used to trace the target and find the distance. The first radar was developed and patented by Huelsmeyer in 1904. Development of Radars was at fast pace during the World War II and in 1930's the earliest experiments were made to detect an aircraft by radars. As the time advanced the applications of radars increased and nowadays these are crucial systems with a range of applications such as detection, surveillance, imaging, navigation, space exploration, whether forecasting, remote sensing, etc...

RADAR Systems work under the principles of electromagnetic wave propagation. When an electromagnetic wave (usually termed as pulse) is transmitted by the radar, it travels with the propagation velocity close to that of the light and backscatters the pulse when something obstructs the course of its propagation. This backscattered pulse is received by the receiver and analyzed in the radar system to detect and find the range and thereby location of the target. The range between the target and the receiver is calculated by the time delay between the transmitted and received pulses by considering the velocity of wave propagation identical to that of light. Time delay could be found by cross-correlating the transmitted and the received pulses. Based on the configuration of the transmitters and receivers, radars are classified as mono-static, bi-static and multi-static. In mono-static radar systems transmitter and receiver are co-located on the same antenna while in bi-static radar systems these are separated and placed at different locations. Multi-static radar systems comprise of separated transmitter and many receivers placed at different locations.

In the radar systems the backscattered pulse power $P_r$ received by the radar receiver is given by the radar equation as:

$$P_r = \frac{P_t G_t G_r \lambda^2 \sigma}{(4\pi)^3 {R_t}^2 {R_r}^2} \tag{1}$$

Where $P_t$ is the power transmitted, $G_t$ and $G_r$ are the gains of the transmitter and receiver antennas respectively, $\lambda$ is the wavelength of the signal, $\sigma$ is the radar cross section (RCS) corresponding to the target, $R_t$ is the distance between the target and the transmitting antenna whereas $R_r$ represents the distance between the target and the receiving antenna. The radar equation for the mono-static radar system is simplified as

$$P_r = \frac{P_t G^2 \lambda^2 \sigma}{(4\pi)^3 R^4} \tag{2}$$

Since $G_t = G_r = G$ and $R_t = R_r = R$ as the transmitter and receiver belong to the same antenna.

### 2.1.1 Chirp Signal

The linear frequency modulated (LFM) signal also called as *chirp* signal is the commonly used transmitted pulse in radars because of its simplicity in generation and processing. In addition to this it has good correlation property because of which pulse resolution is increased using matched filter technique [11]. It is called as LFM signal because of its linear sweep over frequencies like the chirp of a bird. The frequencies in the chirp signal can increase from low to high called as up-chirp or decrease from high to low called as down-chirp. The transmitted chirp signal is given as:

$$S_t(\tau) = rect\left(\frac{\tau}{T_p}\right) e^{2j\pi\left(f_c\tau + \frac{K\tau^2}{2}\right)} \qquad |\tau| \leq \left|\frac{T_p}{2}\right| \tag{3}$$

Where "*rect*" is the rectangular function corresponding to time $\tau$, $T_p$ is the pulse duration, $f_c$ is the centre frequency and K is the chirp rate or LFM rate. From [11] the phase of the signal is represented as:

$$\emptyset(\tau) = \pi K \tau^2 \tag{4}$$

From [11] Instantaneous frequency can be found by calculating the first derivation of $\emptyset(\tau)$.

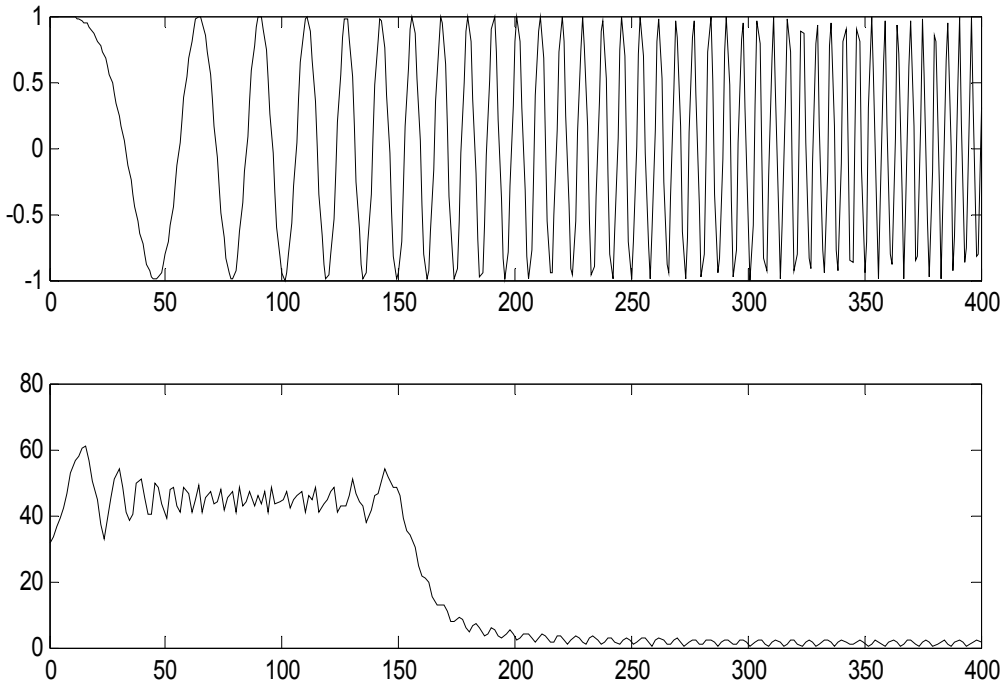


Figure 1: Chirp Signal and its Frequency Spectrum

$$f = \frac{1}{2\pi}\frac{d\emptyset(\tau)}{d\tau} = K\tau \tag{5}$$

From eq. (3) it could be understood that the frequency is the function time $\tau$ and slope of the function depends on chirp rate K.

The echo signal reflected from the target can be represented as:

$$S_r(\tau) = rect\left(\frac{(\tau-\tau_d)}{T_p}\right) e^{2j\pi\left(f_c(\tau-\tau_d)+\frac{K(\tau-\tau_d)^2}{2}\right)} \qquad |(\tau-\tau_d)| \leq \left|\frac{T_p}{2}\right| \tag{6}$$

Where $\tau_d$ is the time delay between the transmitted and received pulse.

$$\tau_d = \begin{cases} \frac{2R}{c}, \text{for monostatic radar} \\ \frac{R_t+R_r}{c}, \text{for bistatic radar} \end{cases}$$

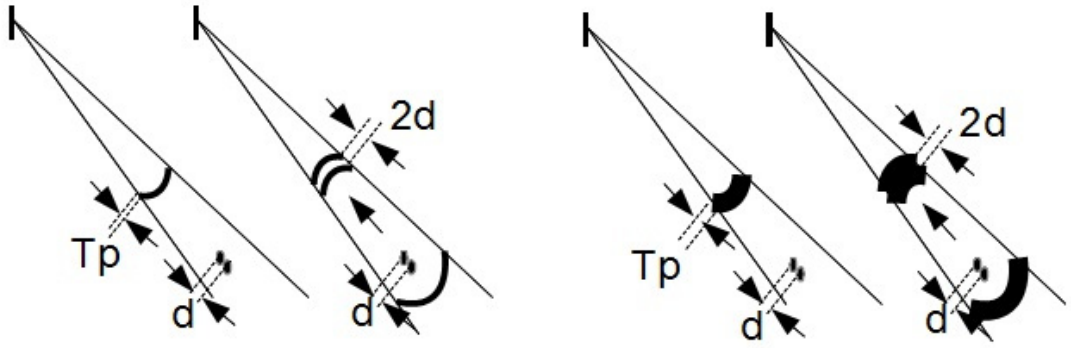


Figure 2: Representation of range resolution of a radar.

### 2.1.2 Radar Resolution

Radar resolution comprises of two parts namely *range* and *azimuth* resolution for two dimensional imaging scenarios. These are also referred as *cross track* and *along track* resolutions.

**Range resolution $R_r$:** It can be described as the ability of the radar system to distinguish between two adjacent targets of different ranges but on the same cross track direction. The efficiency of the range resolution depends upon the dimensions of the target, efficiency of receiver and mainly on the width of the transmitted pulse. It can be given as:

$$R_r = \frac{cT_p}{2} = \frac{c}{2B} \tag{7}$$

Where $c$ is the velocity of light, $T_p$ and $B$ are the time period and bandwidth of the transmitted pulse respectively. It means that if the width of the transmitted pulse is relatively short i.e. $T_p < \frac{2d}{c}$ , the radar can distinguish two adjacent targets close to each other since it receives two distinct echoes as shown in Fig.2. If the pulse width is relatively large i.e. $T_p \geq \frac{2d}{c}$ then the two adjacent targets cannot be distinguished as two but instead their echoes will be mixed and they will appear as a single target at the receiver end.

**Azimuth Resolution $R_{az}$:** It can be described as the ability of the radar system to distinguish between two adjacent targets which are side by side but at same range from radar antenna. The degree of azimuth resolution depends on beam width for detection radars i.e a narrow

beam width antenna will have better $R_{az}$ which can be understood from Fig.3. It is different from the imaging radars where $R_{az}$ is based on the antenna pattern of radar i.e. by the angular aperture at -3dB and the distance between target and radar. According to [12], azimuth resolution is defined by:

$$R_{az} = \theta_{3dB} R \sim \frac{\lambda}{L} R \tag{8}$$

where $R$ is range of the target, $\lambda$ is wavelength of the signal and $L$ is length of antenna. The Pulse Repetition Frequency (PRF) is chosen in such a way that antenna turns by an angle $\theta_{3dB}$ between two pulse emissions. PRF should also be adapted according to $R_{az}$ and platform speed $v$ such that radar travels a distance of $\frac{v}{PRF} = R_{az}$ before sending another pulse [12].

Imaging radars are mainly mounted on aircrafts or satellites and the azimuth resolution is low in these radars since $R_{az}$ depends on antenna length (aperture length) which is considerably small in them. For instance a radar of 6 m long antenna operating in X – band ($\lambda = 3cm$) at a range of 10 km (airborne) will have $R_{az} = 50m$ which is quiet large i.e. not a better resolution since image is formed with each pixel corresponding to 50 m. Thus to improve the resolution very long antennas (apertures) are synthesised which are so called Synthetic Aperture Radars and abbreviated as SAR.

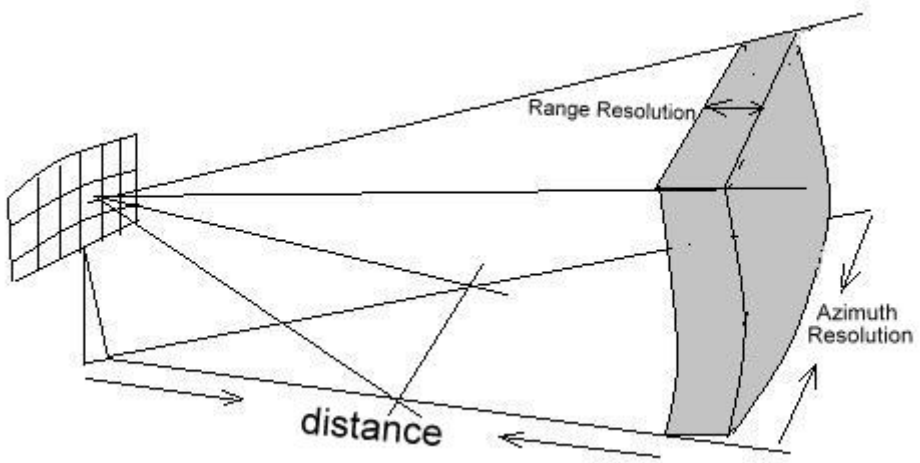


Figure 3: Detection radar showing azimuth and range resolutions.

### 2.1.3 Pulse Compression & Matched Filtering

To achieve better range resolution, a pulse with narrow main lobe is required but pulse with narrow main lobe will have less power and hence the echo of such pulse gets buried in the noise. Thus the receiver may not get the target information and so it is not acceptable to transmit a pulse with narrow pulse. To overcome such issue pulse compression technique is used in which the main lobe of the pulse is narrowed by signal processing. Pulse compression is a common technique used in signal processing which allows increasing SNR and offers solution for the improvement of resolution in the range direction [13].

Pulse compression is performed by matched filtering in which the energy of the signal is compressed into a narrow main lobe which is approximated as a sinc function carrying 90% of total signal energy. Matched filtering is based on the auto correlation of transmitted signal and performed by the convolution between the time reversal conjugate of the transmitted signal (3) and the time delayed received signal (6). It is represented by

$$S_{MF} = S_t^*(\tau) \otimes S_r(\tau) \tag{9}$$

Substituting (3) and (6) in (9) and then simplifying integrals results in

$$S_{MF} = (T_p - |\tau|) rect\left(\frac{\tau}{2T_p}\right) sinc\left[k\tau(T_p - |\tau|)\right] \tag{10}$$

From (10), it can be seen that much of the total signal energy is concentrated in the main lobe of the sinc function there by obtaining pulse of finer resolution having signal energy almost same to that of the transmitted chirp pulse.

### 2.1.4 Interpolation

Interpolation is required to accurately find the sample corresponding to that of the time delay. SAR raw data should therefore be highly sampled to improve accuracy and minimize errors. Received signals are sampled according to the Nyquist rate which is greater than or equal to that of twice the signal bandwidth. Interpolation techniques are used to reconstruct the signal from other samples as well.

Interpolation is used to improve the quality of the image. Different methods are available for interpolation in which nearest neighbour method is the easiest one. Other methods of interpolation are sinc, linear, cubic, quadratic and spline methods. In this thesis nearest neighbour interpolation is used by up sampling the signal.

## 2.2 Synthetic Aperture Radar (SAR)

SAR is a kind of imaging radar which utilizes radio frequencies and hence called as radio sensing system or a sensor. SAR is advantageous over optical imaging sensors because of its operating ability in any kind of climatic conditions irrespective of daylight. Synthetic aperture radars (SAR's) are different from real aperture radars (RAR's) based on the type of apertures. As the name suggests in RAR the aperture is real and depends on the dimensions of the antenna where as in SAR the aperture is not real but synthesized by moving the antenna across the length of the required aperture size and processing the pulses received at every aperture position as shown in Fig.4.

The importance of SAR is the better radar resolution particularly azimuth resolution that it inherits. According to (8), to obtain high azimuth resolution a very long aperture of several 100's of meters is required but it is not feasible to construct such big aperture antenna and thus a long aperture is synthesised by platform's movement and signal coherence which are called SAR's.

In airborne and space borne SAR although the platform is in motion it is assumed to be stationary according to start stop approximation. Pulse is transmitted from every consecutive point called aperture position and echo is received before retransmitting another pulse from another aperture position. Phases of all such echoes could be combined and processed for creating or synthesizing a large aperture antenna which in easy terms mean constructing a large antenna by signal processing techniques. In our GB-SAR system start stop approximation is not required since the antenna is moved to another aperture position only after receiving the echo.

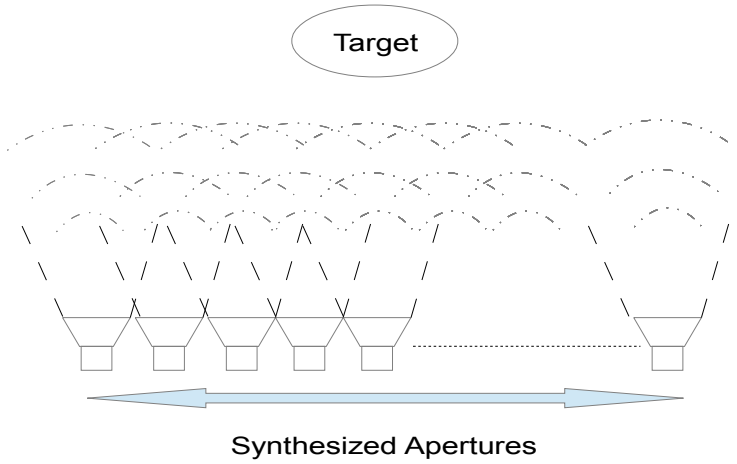


Figure 4: Synthetic aperture radar focussing on target.

### 2.2.1 SAR Geometry

In order to understand the operation of SAR, it is highly required to understand SAR geometry and certain SAR terminologies which are shown in Fig.5 [14].

Target: The area of ground which is being imaged by the SAR.

Cross Range: The axis of the radar platform which is perpendicular to range axis i.e. flight path.

Nadir: The point on the ground which is exactly underneath the SAR platform. In other words it is the point of super imposition of SAR platform on ground.

Swath: The width of the antenna beam footprint.

Slant Range: The range of the target from the SAR platform. Since the range from SAR on the platform to the ground target is slant, it is named as slant range.

Range or Ground Range: The distance from the nadir point to the target. In other words it is the projectile of the slant range.

Beam footprint: The foot print of radar antenna beam on the ground i.e. the area illuminated by the radar antenna beam.

Near and far range: The range from nadir point to the nearest edge of swath and farthest end of swath.

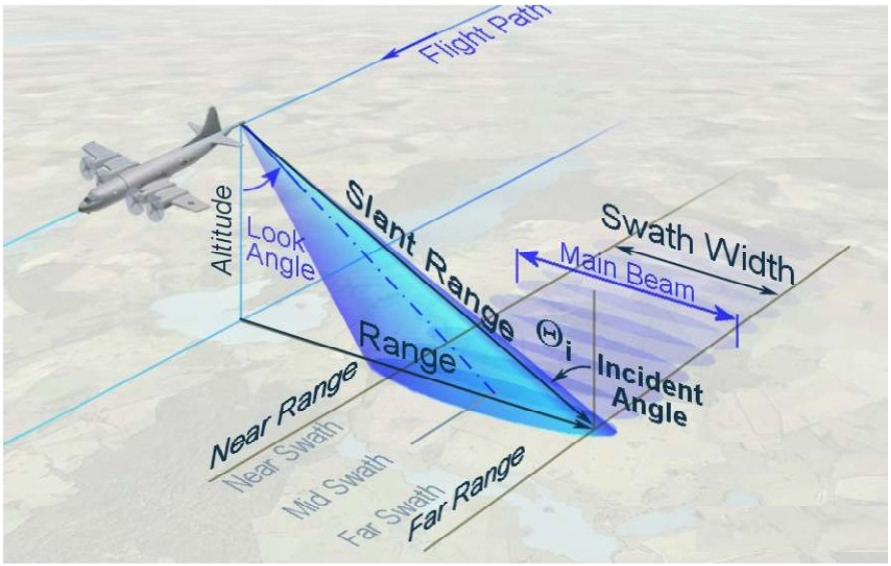


Figure 5: SAR Geometry [14]

Look angle: The angle between slant range and axis perpendicular to ground.

Incident angle: The angle of elevation from target to the SAR platform.

Integration angle: The angle at the target formed by joining target with the first and last aperture positions.

### 2.2.2 Modes of Operation

According to the platform in which SAR systems are installed there are named as air borne systems i.e. placed on aircrafts, space borne systems i.e. placed on spacecrafts or satellites and ground-based systems i.e. installed on ground tracks.

With respect to the directivity of the antenna used and its operational mechanism, SAR is classified into three modes viz. strip map mode, spotlight mode and scan mode. In the strip map mode the area focused by the main beam of antenna changes along with the position of the antenna under movement which means antenna directivity is constant along the motion of the SAR platform. In spotlight mode the area focused by the main beam of the antenna is always constant through the movement of the platform which means antenna directivity changes consistently in order to illuminate the interested area of target. In scan mode the area focused by the main beam of the antenna changes continuously scanning the area of interest at any angle as shown in Fig.6.

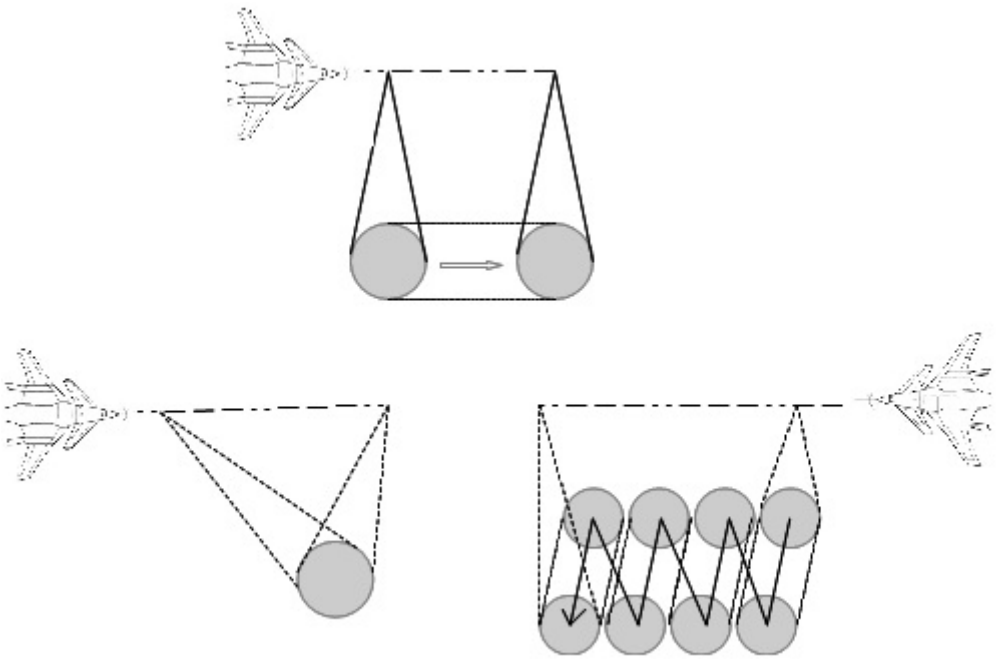

Figure 6: Strip map mode, Spotlight modes and Scan mode of SAR operation.

## 2.3 Ultra Wide Band (UWB-SAR)

Utilizing the foliage & ground penetrating feature of the low frequency electromagnetic waves, UWB-SAR systems are also developed to investigate the earth's crust for geological purposes like remote sensing or to discover objects underneath ground or behind the wall. Such systems are called GP-SAR (Ground Penetration SAR) or FOPEN (Foliage Penetration). Usage of low frequencies has adverse effects on the azimuth resolution. To overcome this drawback, low frequency SAR systems employ ultra-widebeam antennas and for high range resolution they make use of ultra-wideband frequencies. Such systems are called as ultrawideband – ultrawidebeam systems (UWB). These SAR systems with high resolution have the ability to penetrate camouflage and foliage [15]. Few available UWB SAR systems in the world are listed in Table 1.

UWB SAR systems with its advantages give a solution for effective detection of objects or targets under the ground or behind the walls.

| Name of the SAR System | Frequency Band | Frequencies | Fractional Bandwidth |
|---|---|---|---|
| CARABAS - II | Lower VHF Band | 20 – 90 MHz | 1.27 |
| LORA | VHF / UHF | 200 – 800 MHz | 1.20 |
| P-3 | VHF / UHF | 215 – 900 MHz | 1.22 |
| PAMIR | X - Band | 8.0 – 12.5 GHz | 0.43 |
| BoomSAR | VHF / UHF | 50 – 1200 MHz | 1.84 |

Table 1: Various UWB SAR systems and their operating frequencies

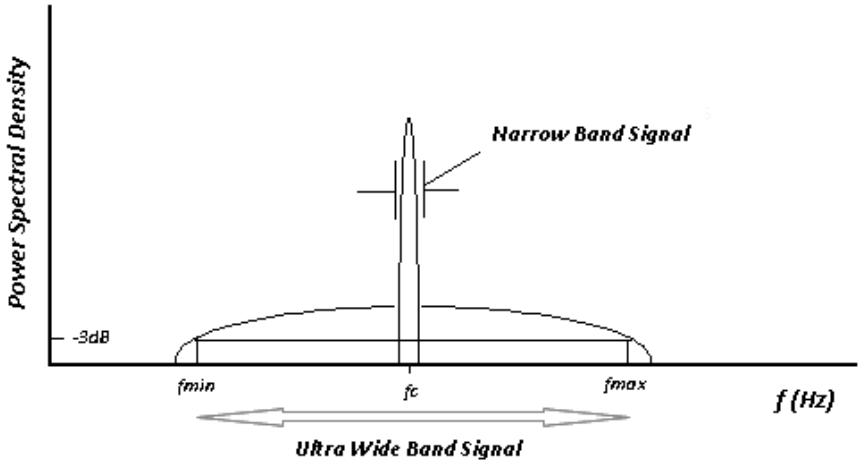


Figure 7: PSD sketch of NB and UWB signals

Regarding the beam width of the antenna corresponding to UWB SAR, an official definition is not yet administered. According to Federal Communications Commission (FCC) any signal with the fractional bandwidth of 0.20 or more is described as UWB signal. Fractional bandwidth $B_r$ is defined by

$$B_r = \frac{f_{max} - f_{min}}{f_c}$$

where $f_{max}$, $f_{min}$ and $f_c$ are the maximum, minimum and central frequencies.

# Chapter 3

# SAR Signal Processing

In the previous chapter, the basics of radar are defined and an overview of synthetic aperture radar is presented. This chapter focuses in detail on the SAR image processing algorithms. The function of these algorithms is to form an image by processing the echo signals received from every aperture position. SAR image processing algorithms are classified as frequency-domain algorithms and time-domain algorithms and both of them have certain pros and cons.

## 3.1 About SAR Algorithms

Frequency-domain algorithms are very well known for their computational efficiency and thus they were widely used in the earlier SAR systems. Basic frequency-domain algorithms are *Range Doppler (RD), Range Migration (RM*) and *chirp scaling (CS).* There are few drawbacks in these algorithms such as:

- Some of them do not support large image size or large integration angle since they contain approximations.
- Implementation of two-dimensional frequency transforms requires large memory for computation.
- Some of them are valid only for linear flight track model which is not always possible especially due to motion errors when large integration angles are used.
- Some of them require very high computational cost for interpolation and it is hard to avoid the errors caused by this processing step.

Because of such drawbacks, frequency-domain algorithms are not recommended in the case of UWB SAR systems [17] [18]. On the other hand we have time-domain algorithms such as global back projection algorithm (GBP), fast back projection (FBP) and fast factorised back projection algorithms (FFBP). The base of all the back projection algorithms is GBP and the

number of computations it takes is higher when compared to its frequency-domain counter parts. However, it is the technique that yields accurate results [16] [19]. Other fast time-domain algorithms like FBP and FFBP make certain assumptions because of which they may not yield accurate results. Computational load of this fast time-domain algorithms is almost similar to frequency-domain algorithms in the case of mono static SAR. In this thesis we use GBP algorithm which yields accurate results and whose computational load depends upon the number of apertures and image size given as $N_A * N_x * N_y$, where $N_A$ represents the number of aperture positions, $N_x$ represents the number of pixels on the image screen along range direction and $N_y$ represents the number of pixels on the image screen along azimuth direction.

## 3.2 Global Back Projection Algorithm

The GBP algorithm was introduced in 1980's and is the base of all the other time-domain algorithms, it is also believed to give high SAR image quality since the algorithm does not generate any phase error. The performance of any other time-domain algorithm is analysed by comparing with the GBP algorithm performance since it yields the accurate results. GBP allows extremely large range migration which is most required in the practical UWB – SAR systems because of imperfect linear motion of the SAR platform. It also accepts any size of SAR image, in simple terms GBP is selected in this thesis because of the merits it inherits.

The GBP algorithm is interpreted as a linear and direct transformation process from radar echo into a complex SAR image. To perform this algorithm, location of the SAR platform and its range from the target image are required. For the operational simplicity SAR image scene is reconstructed on the slant range plane *(x, r)* where *x* represents the azimuth direction and *y* represents the range direction. Since the SAR platform moves in the azimuth direction *x* at any arbitrary time *t* platform moves at a distance of *vt* where *v* is the velocity of platform. Thus PRF should be selected keeping in mind the velocity of the SAR platform. Since pulse compression is the prominent factor for better resolution, let point target be $(x_0, r_0)$ and the received pulse-compressed signal at each aperture position is given by

$$S_{cp}(t,\tau) = e^{2j\pi(f_c(\tau - t_d(t)))}\, 2T_s(t,\tau)\frac{Sin\big(uT_s(t,\tau)\big)}{uT_s(t,\tau)} \quad \tau \in \big[t_d(t) - T_p,\ \ t_d(t) + T_p\big]$$

where *t* and $\tau$ represents azimuth time and range time and

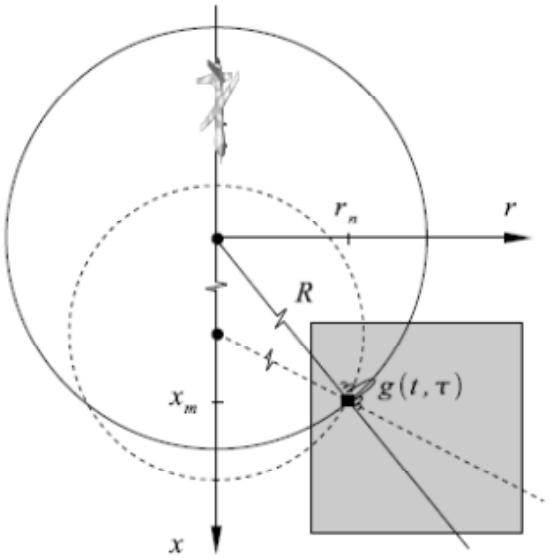


Figure 8: Illustration of GBP Algorithm in monostatic SAR [16].

$$T_s(t,\tau) = \frac{T_p}{2} + \frac{|\tau - t_d(t)|}{2}$$

$$u = 2\tau K(\tau - t_d(t))$$

$$t_d(t) = \frac{2R_0(t)}{c}, R(t) = \sqrt{(x_0 - vt)^2 + {r_0}^2}$$

For a monostatic SAR the superimposition of radar echo for reconstruction of SAR image scene *(x, r)* is represented by [16]

$$Im(x,r) = \int_{\frac{-t_i}{2}}^{\frac{t_i}{2}} S_{cp}\left(t, \frac{2R(t)}{c}\right) dt$$

The Fig. 8 shows the back projection of the pulse compressed signal in the slant plane. It can be seen that the algorithm is carried out in spherical mapping. At every aperture position, the radius of the sphere is given by the range *R*. All the pixels on the image scene along with the range *R* will be mapped by the same data sample. (But we form the SAR image on the ground plane (x,y) not (x,r)).

# Chapter 4

# Ground – based SAR

SAR systems can be classified into categories based on platform of their operation as space borne, airborne and ground-based SAR (GB-SAR) systems. Usually space borne and airborne systems are used for the vast range of applications they support but nevertheless ground – based systems also feature quiet good deal of applications. Additionally GB-SAR systems are utilized for research activities. By utilizing GB-SAR systems during initial phase of research i.e. preliminary research, one could avoid huge expenses caused due to field campaigns [20]. Sometimes SAR raw data is unavailable because of its vast military applications and although SAR raw data is available in few space research websites, the data might not support the requirement of research. In such cases GB-SAR system is highly advantageous with which we can obtain SAR raw data according to the requirement of our research. In this thesis the developed GB-SAR system is utilized to obtain the SAR raw data for circular aperture.

However, GB-SAR systems are also useful in a context when the region of observation is small, in such case using a space borne or airborne systems could be disadvantageous not only in aspect of cost parity but also due to their inefficiency in such cases. Since the airborne and space borne systems operate from quiet large distance, dealing with small area could cause low integration angles there by dropping down the resolution capabilities, causing more interferences and reducing the required SAR scene information. In such cases, GB-SAR could be advantageous which restrain us from undergoing such demerits.

This could be understood from [7] in which they have used a GB-SAR system for monitoring of landslides in Tessina province which is landslide prone area located near the city of Belluno in Italy. The aim of the experiment was to analyze the quality of estimations regarding the displacement of terrain by comparing them with the results provided by their topographic counterparts. The GB-SAR system was placed just at a distance of 500 m allowing the landslide to be observed along the same line of sight corresponding to the topographic device, thereby allowing both the systems to estimate same displacement vector component. Their experiment

concluded that the estimations on both the devices were in good agreement and stressed the use of GB-SAR systems for such applications of landslide monitoring because of their non-invasive property and easiness of use. It was also stressed that GB-SAR systems can be used in unstable zone or cultural heritage monitoring and be benefited from its applications.

In [21], it was described that GB-SAR systems are the efficient techniques for monitoring of widespread areas. In the study, two examples of applications were considered where one is the monitoring of post land slide surface to estimate slope displacements and other is the observation of Tsunami affected area for ground surface movements. Analyses were performed on both the examples which yielded useful information on the distribution of displacement and it was alleged that no such analysis could be performed using conventional methods. One of the best advantages of GB-SAR system is its measurement technique which allows the measurement of displacement. The level of accuracy of the displacement measurement depends on the resolution of the GB-SAR system and thus the best results can be obtained with higher resolution systems. It was also said that these features can only be achieved using GB-SAR technique. The measurement campaign is expected to last until 2017, as there are not many long-term GB-SAR scientific measurements the results of this measurement campaign may help in the better understanding about the dynamics of landslides there by contributing to the mitigation and prevention of natural disasters.

In [22], a GB-SAR system was used for analysis of the growth vegetation. Measurement campaign was made for three seasons and the obtained results showed good agreement with the ground truth. Different components of the trees have different scattering mechanisms and these were demonstrated in this paper using polarimetric analysis techniques. It was also emphasised that the GB-SAR system used can be used as the tool to demonstrate the ground truth for airborne or space borne SAR systems.

In [23], a GB-SAR system was used for the survey of North Eemian (NEEM) Ice drilling site in Greenland. Measurement campaign had been made for 3 weeks and data around 9.7 TB had been collected and processed in which range resolution of 8m and azimuth resolution of 5m was achieved. Results have shown the deepest internal layers which were never imagined in Greenland, this gave more confidence for extracting the ice from the NEEM site. Bed terrain variation was so less for the 100 square-km of area covered around the drill site which means that the ice flow is very little around the site there by leaving the layers undisturbed.

In [24], the monitoring of Alpine Glacier was performed by means of interferometric GB-SAR system. Usually monitoring of glaciers was performed by space borne systems but in the research it was emphasised that the GB-SAR system was used to evaluate the potential of such system in estimating the velocity of unstable area belonging to the glacier. It was concluded that

interferometric maps obtained from the GB-SAR system were able to find the unstable zones and the results were in agreement with the ones obtained from other techniques such as optical sensor measurements.

In [25], monitoring a snow covered slope was done by using GB-SAR Interferometer. Presence of clearly measurable interferometric phase variations corresponding to the variations in the height of snow layer are obtained in the results which showed the ability of ground based systems in such applications.

Apart for these applications, GB-SAR systems are also used in the ground penetrating applications. For example in [5] GB-SAR system in the ultra high frequency range was used for the detection of mines which were buried in the ground and covered by vegetation. It was explained that for such applications SAR could give a better resolution and at low incident angles even the ground clutter is minimized. Thus it can be understood that further increase in resolutions can result in achieving more accurate information.

In [26], a GB-SAR system was used for the detection of residue that blocks the porus media in the oil well due to which the performance of the oil well is reduced. With the early detection of this residue, it can be cleaned thereby increasing the lifetime of the oil well. The results have shown the ability of the GB-SAR system in rendering such applications in oil well maintenance and thereby promoting the system for such kind of applications.

Apart from the applications GB-SAR systems can also be used as a tool for analyzing the functionality of SAR systems by experimenting. Such procedure can restrain from incurring huge expenses which occur due to experimenting on airborne or space borne systems.

# Chapter 5

# Overview of Thesis

The rest of the thesis is divided into three parts.

**Part A**: In the first part, an experimental GB-SAR system is introduced for studying SAR fundamentals. For this purpose, the system is expected to be flexible. This means that the operational frequencies can easily be selected and changed, the length of the aperture can be modified as desired, mode of operation and the aperture can also be modified according to the purpose of research and so on.

According to all these requirements, an experimental GB-SAR system is developed using a vector network analyzer (VNA), a radar antenna and a computer. The process of data acquisition for the developed system is also clearly explained. In order to obtain image clarity suitable number of aperture steps should be used for certain aperture length depending upon integration angle and other parameters, a formula to understand this relation is derived as well. The signal processing method for the acquired data is then described which consists of signal reconstruction and image formation. Then the evaluation about the performance of the GB-SAR system is made based on the assessments of azimuth and range resolutions. The experimentally obtained results are compared with the theoretical assessments to understand the performance of the system.

It was concluded that the comparative results have shown the degradation in both azimuth and range resolution partially caused by the aperture position errors. The considerable mismatch in the azimuth resolution is explained by the artefact of the antenna radiation pattern and SAR strip map mode of operation.

Actual scope of this part of thesis is to develop a GB-SAR system that could be utilized for the advanced research concepts and be instrumental in evolving new technologies. The same system with few required modifications is used in the experimentation section of the second part of this thesis.

**Part B:** This part consists of the importance of the thesis which describes the method for enhancement of image resolution by the usage of circular aperture technique. Firstly the performance of circular aperture SAR system is estimated by executing the theoretic image resolution formulas. The analysis is made by the comparison of obtained results with the results of linear aperture SAR system.

The simulated results were shown and described which clearly show the efficiency of circular apertures over linear apertures. Then the experiment was carried out on GB-SAR system similarly as described in Part A but by changing the aperture to circular, mode of operation and the reflector. Designing of a suitable reflector for the circular SAR experiments was also one of the challenging tasks, because using a normal dihedral corner reflector used for linear aperture will reflect incident wave only from certain directions and thus it is not appropriate for measurements with circular apertures. We proposed and designed a special radar reflector having diamond shape for the experiments.

The measurement results obtained from experiment were in agreement with the theoretical calculations and simulated results. In order to restrain from unmanageable expenses of carrying out field campaigns, the empirical data is obtained from GB-SAR system which in turn signifies the importance of implementing such GB-SAR system in Part A.

After the experimental analysis, the enhancement of resolution is evident from the results obtained and the resolution achieved by CSAR is about 5 times better than that of LSAR ones with the chosen parameter set. However there is a mismatch between the theoretical and practical results which could be an effect due to propagation losses and caused by laboratory environment.

**Part C:** This part consists of few results obtained from the data extracted by the experimental GB-SAR system. These results are provided to give more insight into the impact of aperture parameters on the resolutions and quality of the SAR image. Impact of different SAR modes of operation is also represented with the results. The results of this part could be utilized for the selection of suitable parameters in GB-SAR experiments and broad understanding of the same.

# Conclusion to the thesis

With the advancement and growing applications of SAR technology, enhancement in the resolution of the SAR image is highly anticipated. Enhancement in resolution offers high accuracy in the measurements and SAR image analysis. Therefore in this thesis circular aperture technique is introduced for the improvement of SAR image resolution. To validate real time efficiency of circular aperture, SAR raw data corresponding to circular aperture is required. The work has therefore been divided into two parts as experimental ground-based SAR system for studying SAR fundamentals and resolution enhancement with circular aperture in theory and empirical scenario.

In the first part a ground-based SAR system was built in the laboratory to obtain SAR raw data according to the requirement of the research. An expression for acceptable number of aperture step in GB-SAR system is derived, which is essential to obtain better quality of SAR image. Operation of GB-SAR system and its data processing is explained in detail and SAR image is presented for linear aperture.

In the second part resolution enhancement with circular aperture is focused. A circular aperture is built for using flexible GB-SAR system. A unique structure of corner reflector is built to achieve prominent reflections in CSAR case, since a conventional trihedral reflector cannot support the requirement. Enhancement in the resolution of SAR image is presented with experimental results. In order to verify and evaluate the efficiency and accuracy of the developed SAR system, obtained experimental results are compared with the simulated results and results in theory.

On comparing the results obtained with experimental SAR system for linear aperture and circular aperture, it is observed that circular aperture result shows about five time better resolution than the linear aperture results for SAR image. Since the developed SAR system is flexible it can be utilised to obtain SAR raw data according to the requirement, for any kind of SAR related research.

A technical paper is presented as third part in which few experiments are performed using the developed GB-SAR system to facilitate broad insight into the operations of GB-SAR system for various SAR parameters and different modes of operation.

# References


[1] P. Patel, H. S. Srivastava and R. R. Navalgund, “Use of synthetic aperture radar polarimetry to characterize wetland targets of Keoladeo national park, Bharatpur, India”, in *Current Science*, vol. 97, no. 4, pp. 529–537, 2009.

[2] Srivastava, H.S.; Patel, P.; Sharma, Y.; Navalgund, R.R., "Large-Area Soil Moisture Estimation Using Multi-Incidence-Angle RADARSAT-1 SAR Data," *Geoscience and Remote Sensing, IEEE Transactions on*, vol.47, no.8, pp.2528-2535, Aug. 2009.

[3] Henderson, F.M.; Zong-Guo Xia, "SAR applications in human settlement detection, population estimation and urban land use pattern analysis: a status report," *Geoscience and Remote Sensing, IEEE Transactions on*, vol.35, no.1, pp.79-85, Jan 1997.

[4] J. A. Marble and A. O. Hero, “Phase distortion correction for see through-the-wall imaging radar”, *IEEE ICIP*, Atlanta, GA, pp. 2333–2336, Oct. 2006.

[5] Millot, P.; Berges, A., "Ground based SAR imaging tool for the design of buried mine detectors," The Detection of Abandoned Land Mines: A Humanitarian Imperative Seeking a Technical Solution, EUREL International Conference on (Conf. Publ. No. 431) , vol., no., pp.157,159, 7-9 Oct 1996.

[6] Solberg, A.H.S., "Remote Sensing of Ocean Oil-Spill Pollution," *Proceedings of the IEEE*, vol.100, no.10, pp.2931-2945, Oct. 2012.

[7] N. Casagli, P. Farina, D. Leva, G. Nico and D. Tarchi, “Monitoring the Tessina landslide by a ground-based SAR interferometer and assessment of the system accuracy,” in *Proc. IEEE IGARSS’2002*, vol. 5, Toronto, Canada, Jul. 2002, pp. 2915–2917.

[8] K. Lukin, A. Mogyla, V. Palamarchuk, P. Vyplavin, E. Kozhan and S. Lukin, “Monitoring of St. Sophia Cathedral interior using Ka-band Ground Based Noise Waveform SAR”, *EuMA EuRAD’2009*, Rome, Italy, pp. 215-217, Oct. 2009.

[9] Borner, T.; De Zan, F.; Lopez-Dekker, P.; Krieger, G.; Hajnsek, I.; Papathanassiou, K.; Villano, M.; Younis, M.; Danklmayer, A.; Dierking, W.; Nagler, T.; Rott, H.; Lehner, S.; Fugen, T.; Moreira, A., "Signal: SAR for ice, glacier and global dynamics," *Geoscience and Remote Sensing Symposium (IGARSS), 2010 IEEE International* , vol., no., pp.2884,2887, 25-30 July 2010.

[10] Pierdicca, N.; Rocca, F.; Basili, P.; Bonafoni, S.; Carlesimo, G.; Cimini, D.; Ciotti, P.; Ferretti, R.; Marzano, F.S.; Mattioli, V.; Montopoli, M.; Notarpietro, R.; Perissin, D.; Pichelli, E.; Rommen, B.; Venuti, G., "Synergic use of EO, NWP and ground based measurements for the mitigation of vapour artefacts in SAR interferometry," *Geoscience and Remote Sensing Symposium (IGARSS), 2011 IEEE International* , vol., no., pp.2566,2569, 24-29 July 2011.

[11] M. Soumekh, “Synthetic Aperture Radar Signal Processing with Matlab Algorithms,” John Wiley & Sons, Inc., 1999.

[12] H. Maitre, Processing of Synthetic Aperture Radar Images, ISTE Ltd and John Wiley & Sons, Inc, 2008.

[13] A.G .Stove, “Linear FMCW radar techniques,” Radar and signal processing, IEEE Proceeding F. Vol. 139, No.5, pp.343–350, 1992.

[14] C. Wolff and G. Neubrandenburg, “Radar basics," URL: http://www.radartutorial.eu/18.explanations/ex09.en.html, 2007.

[15] D. Wong and L. Carin, “Analysis and processing of ultrawide-band SAR imagery for buried landmine detection,” IEEE Transactions on Antennas and Propagation, vol. 46, no. 11, pp. 1747-1748, November 1998.

[16] Vu, V.-T.; Sjogren, T.K.; Pettersson, M.I., "Fast backprojection algorithm for UWB bistatic SAR," Radar Conference (RADAR), 2011 IEEE , vol., no., pp.431,434, 23-27 May 2011

[17] V. Vu, T. Sjogren and M. Pettersson, "A comparison between fast factorized backprojection and frequency-domain algorithms in UWB low frequency SAR," in *Proc. IEEE IGARSS'2008*, Boston, MA, Jul.2008, pp. 1293–1296.

[18] L. Ulander, H. Hellsten and G. Stenström, "Synthetic-aperture radar processing using fast factorized back-projection," *IEEE Transactions on Aerospace and Electronic Systems,* vol. 39, pp. 760-776, 2003.

[19] Y. Yang, Y. Pi and R. Li, "Back Projection Algorithm for Spotlight Bistatic SAR Imaging," in *Radar, 2006. CIE '06*, 2006.

[20] Dheeraj N. Nehru, Viet T. Vu, Thomas K. Sjögren and Mats I. Pettersson, “An experimental ground-based SAR system for studying SAR fundamentals”, in *Proc. APSAR 2013*, Tsukuba, Japan, Sep. 2013, pp. 1–4.

[21] Takahashi, K.; Matsumoto, M.; Sato, M., "Continuous Observation of Natural-Disaster-Affected Areas Using Ground-Based SAR Interferometry," *Selected Topics in Applied Earth Observations and Remote Sensing, IEEE Journal of*, vol.PP, no.99, pp.1-9, 2103.

[22] Zheng-Shu Zhou; Hamasaki, T.; Sato, M.; Boerner, W.-M., "3-D broadband ground-based polarimetric SAR data processing for the monitoring of vegetation growth variations," *Geoscience and Remote Sensing Symposium, 2004. IGARSS '04. Proceedings. 2004 IEEE International*, vol.2, no., pp.1248,1251, 20-24 Sept. 2004.

[23] W. Blake, C. Leuschen, C. Laird and D. Dahl-Jensen, “Ground based SAR survey of Basal interface at NEEM drill site,” in *Proc. IEEE IGARSS'2009*, vol. 2, Cape Town, South Africa, Jul. 2009, pp. 594– 597.

[24] Luzi, G.; Pieraccini, M.; Mecatti, D.; Noferini, L.; Macaluso, G.; Tamburini, A.; Atzeni, C., "Monitoring of an Alpine Glacier by Means of Ground-Based SAR Interferometry," *Geoscience and Remote Sensing Letters, IEEE* , vol.4, no.3, pp.495,499, July 2007.

[25] Luzi, G.; Noferini, L.; Mecatti, D.; Macaluso, G.; Pieraccini, M.; Atzeni, C.; Schaffhauser, A.; Fromm, R.; Nagler, T., "Using a Ground-Based SAR Interferometer and a Terrestrial Laser Scanner to Monitor a Snow-Covered Slope:

Results From an Experimental Data Collection in Tyrol (Austria)," *Geoscience and Remote Sensing, IEEE Transactions on* , vol.47, no. 2, pp.382,393, Feb. 2009.

[26] D. Oloumi, P. Mousavi, M.I.Pettersson, D. Elliott, "Detection of Near-Wellbore Formation Damage using Synthetic Aperture Radar", IEEE Transactions on Geoscience and Remote Sensing, submitted for publication.

[27] Vu, V. T.; Sjogren, T.K.; Pettersson, M.I., "On Synthetic Aperture Radar Azimuth and Range Resolution Equations," *Aerospace and Electronic Systems, IEEE Transactions on* , vol.48, no.2, pp.1764,1769, APRIL 2012

[28] Yamada, T.; Yamada, H.; Yamaguchi, Y., "Fundamental study on resolution enhancement of three-dimensional imaging in SAR tomography," *Antennas and Propagation (ISAP), 2012 International Symposium on* , vol., no., pp.624,627, Oct. 29 2012-Nov. 2 2012

[29] Preiss, Mark; Goh, Alvin S., "Coherent Processing of Bistatic and Monostatic SAR Imagery for Range Resolution Enhancement," *Synthetic Aperture Radar (EUSAR), 2010 8th European Conference on* , vol., no., pp.1,4, 7-10 June 2010

# Part I

## “An Experimental Ground-based SAR System for Studying SAR Fundamentals”

# Part I:

Viet T. Vu, Dheeraj N. Nehru, Thomas K. Sjögren and Mats I. Pettersson, “An experimental ground-based SAR system for studying SAR fundamentals”, in *Proc. APSAR 2013*, Tsukuba, Japan, Sep. 2013, pp. 1–4.

# An Experimental Ground-based SAR System for Studying SAR Fundamentals

Viet T. Vu, *Member, IEEE,* Dheeraj N. Nehru, *Student member, IEEE,* Thomas K. Sjögren, *Member, IEEE,* and Mats I. Pettersson, *Member, IEEE*

**Abstract**

The paper introduces a simple experimental ground-based SAR system for studying SAR fundamentals. The SAR system is developed on a vector network analyzer (VNA), for example Agilent E5071C, with some useful built-in functions such as transform and gating. The procedure of acquiring the data by using the SAR system is presented in details. The acquired empirical data is also used to reconstruct the illuminated scene. The possibilities to use the SAR system to support SAR research topics are also discussed in this paper.

**Index Terms**

Ground-based SAR, system development, signal processing

## I. Introduction

SYNTHETIC Aperture Radar (SAR) is a radar system which utilizes small aperture but has ability to synthesize very large apertures by dragging the small aperture antenna through a long distance while recording radar echoes at certain positions and then processing the recorded data. SAR systems are classified by space-borne, air-borne and ground-based depending on the platforms that incorporate those systems. According to this classification, the SAR systems such as RISAT-1 of Indian Space Research Organization (ISRO), ALOS of Japanese Space Exploration Agency (JAXA) and RADARSAT-2 of Canadian Space Agency (CSA) integrated with the satellites belong to the space-borne group while LORA and CARABAS of Swedish Research Defence Agency (FOI) carried by the aircrafts are the examples of air-borne systems. In the simplest case, the synthetic aperture of a SAR system can be fabricated on a ground track. This corresponds to the last classification, i.e. ground-based. One example of ground-based SAR systems is MCRDS developed for survey at the NEEM site in Greenland operating in the VHF frequency band [1]. Another example is LISA developed by Joint Research Centre (JRC) of Italy operating in the Ku, C and L frequency bands for monitoring the landslide [2].

One of the most crucial applications of SAR is high resolution imagery. In comparison to other imaging systems, SAR has advantages like operating ability irrespective of climatic conditions and day light, thereby exploiting the advantages of radio waves. The resolutions (both azimuth and range) of a SAR system can be enhanced by increasing the fraction bandwidth of the radar signal and/or prolonging the integration time of that SAR system. Such kind of SAR system is known as ultrawideband-ultrawidebeam system. Beside this, the applications of SAR can be found in environmental monitoring, surveillance, remote sensing, and navigation. For example, SAR is used in a wide range of environmental applications such as monitoring crop characteristics, deforestation, ice flows and oil spills. Apart from civilian use, the applications such as ground moving target indication (GMTI), change detection and surveillance are developed on SAR. There are also SAR applications like see-through-the-wall for behind wall detection [3] which is very effective with ground-based SAR systems. The reason is the penetration of radio waves into the wall is not much fruitful from air-borne or space-borne SAR systems. Monitoring of hill slides and land slides [4] and monitoring of monuments [5] are other examples of applications relied on ground-based SAR systems.

The unavailability of SAR data for research is the major issue to be addressed. It is quite difficult to acquire the data required for research in the practical scenarios since the mostly available SAR systems both air-borne and space-borne are operated for military applications. Although little data corresponding to civilian applications is available for research on few space agency websites, it may not support the requirements of researchers sometimes. Such demands can be fulfilled with the purposed field campaigns. However, the cost to carry out a measurement campaign is not always managed. This crisis might be solved by a simple experimental ground-based SAR system.

The objective of the paper is to introduce a simple experimental ground-based SAR system for studying SAR fundamentals. For this purpose, the system is expected to be flexible. This means that the operating frequency range of the system can easily be selected, the length of the synthetic aperture can be changed as desired, the features of the synthetic aperture can simply be modified according to the purpose of the research, the operation mode of the system can be stripmap or spotlight, and so forth.

V. T. Vu, D. N. Nehru and M. I. Pettersson are with the Department of Electrical Engineering, Blekinge Institute of Technology, Karlskrona, 37143 Sweden e-mail:viet.thuy.vu@bth.se.

The manuscript is accepted for publication in APSAR 2013, Tsukuba, Japan, September 2013.

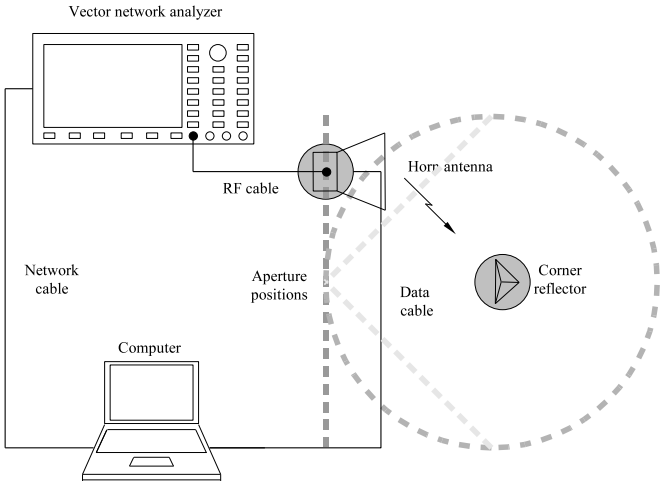


Fig. 1. The system diagram of a simple experimental ground-based SAR system.

The rest of this paper is organized as follows. Section II introduces the simple experimental ground-based SAR system developed on a vector network analyzer (VNA). The procedure for the data acquisition is presented section III. The roles of the functions built-in a VNA such as transform and gating is also presented in this section. Section IV shows SAR scene reconstructed from the acquired empirical data using the SAR algorithms. Applying the introduced ground-based systems to further studies of the SAR fundamentals is discussed in section V. Section VI provides the conclusions.

## II. Developed experimental SAR System

Fig. 1 shows the system diagram of the developed experimental SAR system. The components of the system include a vector network analyzer, an antenna, an antenna positioning and a computer. They are connected together by different kinds of cable.

For the flexibility in selecting of operating frequency range of the SAR system, the VNA should work in a wide frequency range. For example, E5071C - a VNA manufactured by Agilent has system dynamic range from 300 kHz to 20 GHz. Such a dynamic range covers almost all radar bands. Some functions such as transform and gating built-in E5071C are also very useful for SAR system development. These functions will be presented in detail in the next section. E5071C has four ports and allows us to build a bistatic or multistatic ground-based SAR system. The antenna should be an ultrawideband antenna instead of using different narrowband antennas. In this case, a horn antenna is a good selection. A double ridge guide horn antenna manufactured by A.H. system can operate in quite wide frequency range. For example, the frequency range of a double ridge guide horn antenna can be in the range of 700 MHz - 18 GHz and the ground-based SAR system can therefore be configured as an UHF system or even a Ku system. The beamwidth of the antenna is also another consideration. The beamwidth of a double ridge guide horn antenna is wide enough to be used for investigating ultrawideband-ultrawidebeam SAR systems. Hence, its half power beamwidth (HPBW) is up to $48^o$.

For the flexibility in the length of the synthetic aperture and the features of the synthetic aperture, we propose to use a randomly movable tripod. To position the antenna, we can use the indoor GPS device with high accuracy, the marker function embedded in VNA or even position the antenna manually. This allows us to drag the antenna along an unlimited aperture, which is necessary for ultrawideband-ultrawidebeam SAR system investigations. With the use of randomly movable tripod, the aperture of the system can be synthesizing as desired. As shown in Fig. 1, the synthetic aperture can be linear, double linear or circular. Double linear apertures are recently used in the SAR ground moving target indication (GMTI) application [6] while circular apertures are quite popular in high resolution and three-dimension (3-D) SAR imaging [7].

A computer can be used for controlling data acquisition but it is not necessary since the modern VNAs in general and E5071C in particular are computer-based equipments. Storing antenna positions and ground-based SAR data and then processing the data are the more important roles of the computer.

## III. Data Acquisition

In this section, we present the data acquisition with the developed ground-based SAR system. Table I summaries the system parameters and the settings for the experiment.

### *A. System configuration*

The operating frequencies of the ground-based system are selected in the range of 1.5 GHz - 2.5 GHz. The fractional bandwidth is therefore 0.5 which is double of the lower limit of UWB signal, i.e. 0.25. With this operating frequency range,

TABLE I
PARAMETERS FOR GROUND-BASED SAR SYSTEM.

| Parameter | Setting |
|---|---|
| The highest processing frequency | 2.5 GHz |
| The lowest processing frequency | 1.5 GHz |
| Altitude of the ground-based SAR system | 1.25 m |
| Minimum range | 2.86 m |
| Aperture step | 0.05 m |
| Number of aperture positions | 71 |
| Synthetic aperture length | 3.5 m |
| Integration angle | $72^{o}$ |

the far filed condition can easily be fulfilled by a double ridge guide horn antenna. The antenna is horizontally polarized and in this case the antenna HPBW is $48^{o}$. The altitude of the antenna is 1.25 m with respect to the floor level. Table 1 summarizes the parameters of the developed ground-based SAR system.

### *B. SAR scene*

An indoor environment particularly a laboratory which is full of electronic equipments is selected as the SAR scene for data acquisition. A corner reflector 30×30×30 cm is located close to the antenna and placed directly on the floor of the laboratory. Although the dimension of the corner reflector is not optimum for the selected frequency range its reflection is still significant. The minimum range between the corner reflector and the antenna is estimated to be 2.86 m and this separation meets the demand of the far field.

### *C. Synthetic aperture*

The aperture step, i.e. the space between two adjacent aperture positions, and the aperture length depend strongly on the system parameters such as operating frequency range, integration angle associated with antenna beamwidth, and speed of the platform in the cases of airborne and spaceborne. In these specific cases, it is common knowledge that Pulse Repetition Frequency (PRF) of a SAR system must not be chosen less than two times the maximum Doppler frequency to avoid possible aliasing where the maximum Doppler frequency can be estimated by [8]

$$f_D = \frac{2v_{pl}}{\lambda_{min}} \sin\left(\frac{\varphi_{max}}{2}\right) \tag{1}$$

where $\lambda_{min}$ is the wavelength corresponding to the highest frequency of SAR system, $\varphi_{max}$ is the maximum integration angle, and $v_{pl}$ is the velocity of the radar platform. For the case of ground-based SAR system, we can still use (1) as a method to decide aperture step to avoid aliasing. The condition of PRF can thus be written as

$$\text{PRF} \geq \frac{4v_{pl}}{\lambda_{min}} \sin\left(\frac{\varphi_{max}}{2}\right) \tag{2}$$

If we divide both sides of (2) by $v_{pl}$, the following expression will be obtained

$$\frac{\text{PRF}}{v_{pl}} \geq \frac{4}{\lambda_{min}} \sin\left(\frac{\varphi_{max}}{2}\right) \tag{3}$$

The ratio of PRF to $v_{pl}$ on the left hand side of (3) is nothing else than the inverse of aperture step $\Delta L$. The condition for aperture step is therefore formulated by

$$\Delta L \leq \frac{\lambda_{min}}{4} \left[\sin\left(\frac{\varphi_{max}}{2}\right)\right]^{-1} \tag{4}$$

Since integration angle of a SAR system is associated with the antenna beamwidth of that SAR system, it is not appropriate to select an integration angle larger than the first null beamwidth (FNBW) of the antenna. The FNBW of the double ridge guide horn antenna is shown to be up to approximately $180^{o}$. In our data acquisition, the maximum integration angle is chosen by about $\varphi_{max} = 72^{o}$, i.e. one and a half times more than the HPBW of the double ridge guide horn antenna. Based on the operating frequency of the system and the selected maximum integration angle, the aperture step is selected by $\Delta L = 0.05$ m which is compelling with equation (4). According to the information of the SAR scene (location of the corner reflector), the maximum integration angle corresponds to an aperture length of 3.5 m. The number of aperture positions will therefore be 71.

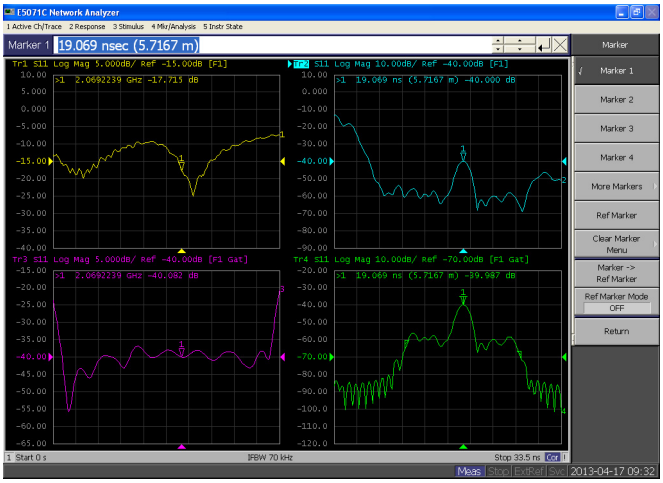


Fig. 2. Data acquisition with the simple experimental ground-based SAR system.

### *D. Data acquisition*

The modus operandi of the ground-based SAR system is the stripmap mode. In the stripmap mode, the antenna is only translated but not rotated during the measurement. In other words, the antenna radiation in directions is kept unchanged regardless of the linear movement of the antenna. This results in a swath along the SAR scene parallel to the path of motion. However, due to the wide antenna beamwidth, the corner reflector is still kept within the mainbeam without steering the antenna. This makes the modus operandi similar to the spotlight mode for the corner reflector.

Fig. 2 shows the data acquisition with the developed ground-based SAR system at an aperture position. As mentioned, the SAR scene for the data acquisition is an indoor environment particularly a laboratory which is full of electronic equipments and the corner reflector is located in the center of the SAR scene. The plot in the upper left corner of the figure (Trace 1 - yellow) shows the measurement of the scattering parameter $S_{11}$, i.e. reflection. The transformation of S11 to time-domain using the transform function built-in VNA is given in the upper right corner (Trace 2 - cyan). The reflection of the corner reflector in the center of the SAR scene can be observed and marked by $\nabla$ using Marker 1. The reflections of other electronic equipments in the laboratory can also be seen from Trace 2. Assuming that a small SAR scene surrounding the corner reflector (e.g. about 2.56$\times$2.56m) is desired to reconstruct. We can use the embedded gating function to select this specific range. The gating function also suppresses the reflections outside the range of interest. The result obtained with the gating function is plotted in the lower right corner (Trace 4 - green). The span of the gate is marked by two small right triangles with respect to the center of the gate marked by $\top$) and not more than 5.12m. The plot in the lower left corner displays the transformation back to frequency domain of this result, i.e. the modified version of $S_{11}$ (Trace 3 - magenta). This version of $S_{11}$ is the data acquired with the system at one aperture position and saved to the computer. Please note that the data can be saved in different formats as desired with the VNA. For our case, we save the data in complex format which comprises of real and imaginary data. This process is repeated for all the aperture positions.

In this experiment, we have totally 71 aperture positions. The data recorded and saved to the computer at every aperture position will then be utilized for SAR scene reconstruction.

## IV. Signal Processing

In this section, the signal processing steps for the acquired data are presented. As summarized in the data acquisition in the previous section, the data is the gated (in time-domain) version of $S_{11}$ (not $S_{11}$) recorded at 71 aperture positions. To get the image of the SAR scene from the recorded data, two signal processing steps - radar signal reconstruction and SAR image formation - are required.

### *A. Radar signal reconstruction*

Since the recorded data contains only the gated version of $S_{11}$ in the selected frequency range, i.e. 1.5 GHz - 2.5 GHz, it is necessary to perform zero padding for other frequencies in radar signal reconstruction. If the sampling frequency is selected by the Nyquist frequency, i.e. 5 GHz, the zero padding is applied to the frequencies in the ranges 0 Hz - 1.5 GHz and 2.5 GHz - 5 GHz. Fig. 3.a shows the gated version of $S_{11}$ recorded at an arbitrary aperture position after zero padding, i.e. the Fourier transform of the radar signal in frequency-domain.

The radar signal is reconstructed with an inverse Fourier transform of the gated version of $S_{11}$ after zero padding. Fig. 3.b shows the reconstructed radar signal. For convenience, the vertical axes in Fig. 3.a and .b are normalized.

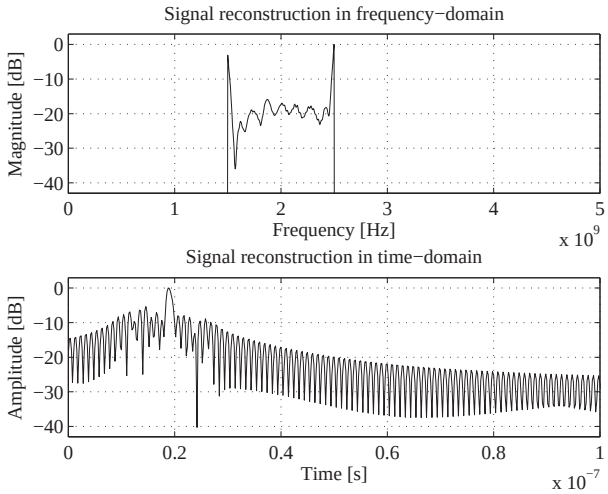


Fig. 3. Radar signal reconstruction from the recored data (a) the gated (in time-domain) version of $S_{11}$ after zero padding in frequency-domain. (b) the inverse Fourier transform of the gated version of $S_{11}$ after zero padding in time-domain.

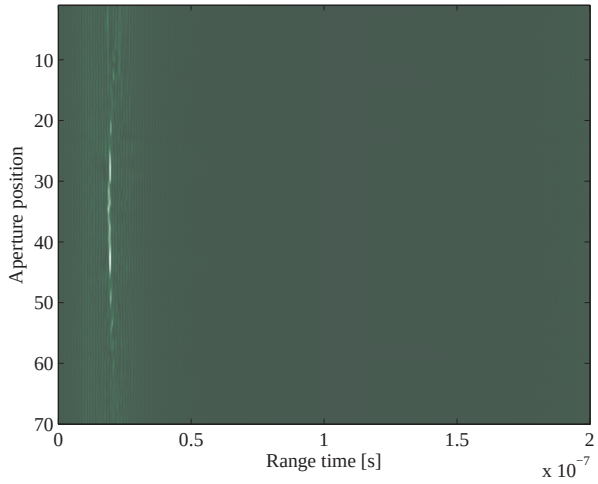


Fig. 4. Radar signal matrix.

The procedure for radar signal reconstruction is applied to all data recorded at 71 aperture positions. Fig. 4 shows the radar signal matrix. The vertical axis corresponds to the aperture positions while the horizontal axis represents the range time. The range migration can be seen from the curve in Fig. 4. The minimum range corresponds to the center aperture position while the maximum range is associated with the first and the last aperture positions. The attenuation with respect to the range, i.e. following the radar equation, can partially be observed since the attenuation is also affected by the radiation pattern of double ridge guide horn. We can also recognize the reflections from other objects in the laboratory at the ten first and the ten last aperture positions.

### *B. SAR image formation*

SAR image formation is relied on SAR algorithms. In this study, we use the Global Backprojection (GBP) algorithm [9] to avoid the phase errors which can be generated by SAR algorithm. Hence, GBP is a time-domain algorithm, has ability to handle extreme range migration, manages large motion error compensation, and has flexibility in selecting SAR scene area. Although the algorithm requires a large computational load, it does not matter for the small number of aperture positions (71 aperture positions) and the small SAR scene area ($2.56\times2.56$ m) in the experiment.

In SAR image formation, the image sample is defined by ($0.01\times0.01$ m). For the SAR scene area of $2.56\times2.56$ m, the number of image samples is $256\times256$ samples. To increase the accuracy of the backproject in GBP, the radar signals are upsampled with a upsampling rate of three using FFT/IFFT. Fig. 5 shows the image of the SAR scene where the corner reflector appears in the middle as a point target. Other objects which cannot be totally suppressed by the gating function of VNA can also be seen in the SAR image.

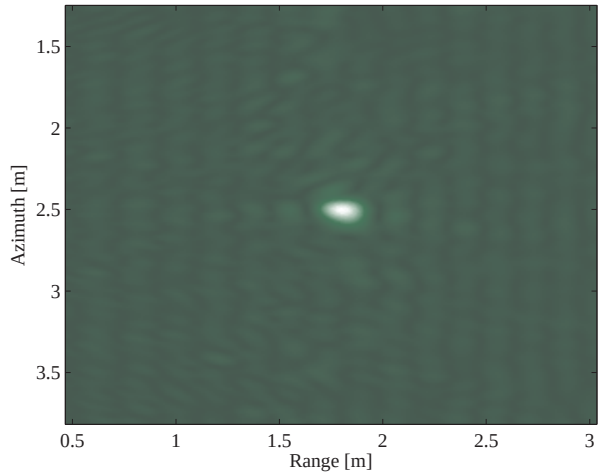


Fig. 5. SAR image of the illuminated scene.

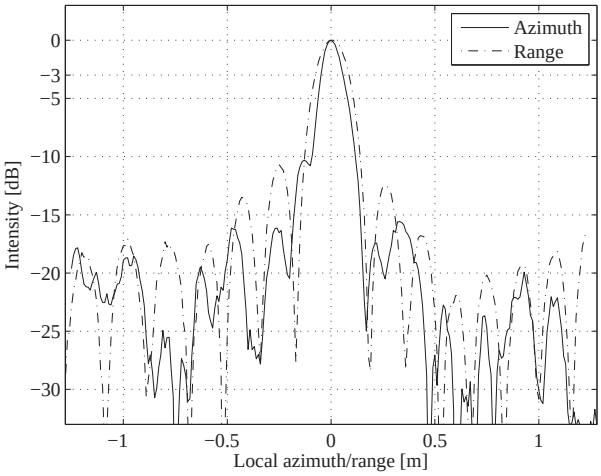


Fig. 6. Azimuth and range vectors extracted from the peak intensity of the SAR image in Fig. 5 (the center of the SAR image). The horizontal axis is regulated to the local azimuth and range instead of using the true azimuth and range.

### *C. Evaluation*

It is common knowledge that the evaluations about the performance of a SAR system are based on the assessments such as azimuth resolution, range resolution, Integrated Sidelobe Ratio (ISLR) and Peak Sidelobe Ratio (PSLR). Among them, azimuth and range resolutions are considered to be the most significant parameters since they describe the distance between two objects on the ground so that these objects appear distinct and separate in a SAR image. The plots of the azimuth and range vectors extracted from the peak intensity of the SAR image in Fig. 5 are given in Fig. 6. In Fig. 6, the horizontal axis is regulated to the local azimuth and range instead of using the true azimuth and range while the vertical axis is normalized. The plotted vectors are the bases for the azimuth and range resolution measurements. The measured results are 0.10 m in azimuth and 0.16 m in range.

If we use resolution equations proposed in [10] to estimate the azimuth and range resolutions, the results will be 0.05 m in azimuth and 0.14 m in range. This indicates that both the azimuth and range resolutions obtained with the experiment are worse than the ones in theory. The degradation in resolutions are partially caused by the small aperture position errors. Such errors are very sensitive when the antenna and the corner reflector are located close together. However, the resolution in range is quite close to the measurement result indicating the good performance of the experimental ground-based SAR system. The measured azimuth resolution is much worse than the estimated one. This can be explained by the low efficiency of the integration angle in the stripmap mode which depends strongly on the antenna radiation pattern or in other words the antenna beamwidth. This means that only a certain number of aperture positions in the center contribute to the azimuth focusing of the corner reflector. The data matrix given in Fig. 4 where the strong reflection from the corner reflector can only be observed

in the middle part of the matrix (from the aperture position 20 to the aperture position 50) clearly illustrates this.

## V. Conclusion

In this paper, we introduce the simple experimental ground-based SAR system. The procedure of data acquisition incorporating with the SAR fundamentals are also emphasized. The processing steps - radar signal reconstruction and image formation - for the data recorded by the experimental system are also explained in detail. The SAR image formed with the experimental data is examined, measured and compared with the assessments in theory. The comparative results show the degradation in both azimuth and range resolutions partially caused by caused the aperture position errors. The considerable mismatch in the azimuth resolution is explained by the artifact of the antenna radiation pattern.

The experimental system introduced in this paper can be utilized further in research of more advanced topics related to SAR. One of the possible research is an experimental study for the enhancement of SAR image resolution by using circular apertures. The system can also seen to be basis for developing other SAR systems. For example, with the number of ports available on VNA, it is possible to develop a experimental ground-based bistatic SAR system.

## Acknowledgment

The authors would like to thank the KK-Foundation for making this research project possible, and are also appreciative of support from the Swedish Defence Research Agency, Saab Bofors Dynamics, Saab Microwave Systems and RUAG Space.

## References

[1] W. Blake, C. Leuschen, C. Laird and D. Dahl-Jensen, “Ground based SAR survey of Basal interface at NEEM drill site”, in *Proc. IEEE IGARSS’2009*, vol. 2, Cape Town, South Africa, Jul. 2009, pp. 594–597.

[2] N. Casagli, P. Farina, D. Leva, G. Nico and D. Tarchi, “Monitoring the Tessina landslide by a ground-based SAR interferometer and assessment of the system accuracy”, in *Proc. IEEE IGARSS’2002*, vol. 5, Toronto, Canada, Jul. 2002, pp. 2915–2917.

[3] J. A Marble and A. O. Hero, “Phase distortion correction for see-through-the-wall imaging radar”, *IEEE ICIP*, Atlanta, GA, pp. 2333–2336, Oct. 2006.

[4] M. Pieraccini, G. Luzi, D. Mecatti, L. Noferini and C. Atzeni, “Ground-based SAR for short and long term monitoring of unstable slopes”, *EuMA EuRAD’2006*, Manchester, UK, pp. 92–95, Sep. 2006.

[5] K. Lukin, A. Mogyla, V. Palamarchuk, P. Vyplavin, E. Kozhan and S. Lukin, “Monitoring of St. Sophia Cathedral interior using Ka-band Ground Based Noise Waveform SAR”, *EuMA EuRAD’2009*, Rome, Italy, pp. 215-217, Oct. 2009.

[6] V. T. Vu, T. K. Sjögren and M. I. Pettersson, “Ground moving target detection and estimation with different SAR linear flight tracks”, in *Proc. IEEE IGARSS’2013*, Melbourne, Australia, accepted for publication, Jul. 2013.

[7] V. T. Vu, T. K. Sjögren and M.I. Pettersson, “Studying CSAR systems using IRF-CSAR”, in *Proc. IET RADAR*, Glasgow, UK, Oct. 2012, pp. 1–6.

[8] V. T. Vu, T. K. Sjögren and M.I. Pettersson, “Ultra-wideband chirp scaling”, *IEEE Geosci. Rem. Sens. Lett.*, vol. 7, no. 2, pp. 282–286, 2010.

[9] L. E. Andersson, “On the determination of a function from spherical averages”, *SIAM Journal on Mathematical Analysis*, vol. 19, no. 1, pp. 214–232, 1988.

[10] V. T. Vu, T. K. Sjögren and M. I. Pettersson, “On synthetic aperture radar azimuth and range resolution equations”, *IEEE Trans. Aerosp. Electron. Syst.*, vol. 48, no. 2, pp. 78–83, 2012.

# Part II

## "SAR Resolution Enhancement with Circular Aperture in Theory and Empirical Scenario"

# Part II:

Dheeraj N. Nehru, Viet T. Vu, Thomas K. Sjögren and Mats I. Pettersson, “SAR resolution enhancement with circular aperture in theory and empirical scenario”, *submitted to Proc. IEEE RadarCon 2014*, Cincinnati, USA, May 2014.

# SAR Resolution Enhancement with Circular Aperture in Theory and Empirical Scenario

Dheeraj N. Nehru*, *Student member, IEEE,* Viet T. Vu*, *Member, IEEE,* Thomas K. Sjögren, *Member, IEEE,* and Mats I. Pettersson, *Member, IEEE*

**Abstract**

SAR systems synthesizing circular apertures have been shown to result in better spatial resolutions than the ones synthesizing linear apertures. The paper presents an investigation about the enhancement of SAR spatial resolutions with the use of circular aperture. A comparison between the spatial resolutions obtained with a SAR system synthesizing a circular aperture and with the same SAR system synthesizing a linear aperture is therefore carried out. The studying results are verified by the experimental SAR data set provided by the experimental ground-based SAR system of Blekinge Institute of Technology (BTH GB-SAR).

**Index Terms**

Ground-based SAR, linear aperture, circular aperture, resolution

## I. Introduction

SYNTHETIC Aperture Radar (SAR) is a radar sensor system which allows high resolution imagery and inherits advantage of usability in any environment because of its operating ability irrespective of severe climatic conditions and daylight. SAR is described as a system which assumes large aperture by synthesizing from the linear movement of radar platform. The requirement for high resolution images is inevitable due to the growing applications of SAR systems. For example, forest vegetation analyses using SAR will be more accurate with the enhanced resolution images [1]. Let it be any kind of monitoring applications such as monitoring monument or landslides or hill slides, utilization of high resolution SAR imagery always yields accurate results [2]. This requirement is the motivations for researchers to develop novel strategies for the resolution enhancement of SAR images.

In order to improve the resolution of SAR images increasing the integration angle and the center frequency of a SAR system and/or using the wider signal bandwidth are the main solutions. Using the wider signal bandwidth for a SAR system can lead to some challenges. For example, that SAR system has a higher possibility to be affected by radio frequency interference (RFI) caused by other radio systems on the ground scene. Increasing the center frequency for a SAR system causes a greater propagation loss and difficulties of generating and amplifying the signal energy. Using a higher integration angle can be a better option but this option depends strongly on the antenna beamwidth utilized by a SAR system. In addition, for a linear aperture, the maximum integration angle is always less than $180^{o}$. To increase integration angle, a strategy has been introduced in [3], [4] which suggest the use of circular apertures. This strategy has been shown as a method to enhance SAR resolution.

The spatial resolutions, which can be obtained with a SAR system in theory, have been investigated in [5], [6]. For a SAR system synthesizing linear aperture (LSAR), the azimuth resolution is shown to be dependent on the integration angle, the center frequency and the so-called azimuth/range coupling factor in azimuth of that SAR system whereas the range resolution is inversely proportional to the radar signal bandwidth and proportional to the azimuth/range coupling factor in range. The mentioned azimuth/range coupling factors are show to be the functions of fractional bandwidth and integration angle. For a SAR system synthesizing circular aperture (CSAR), the unique spatial resolution depends on the radar signal bandwidth and another factor which is defined by the fractional bandwidth and the incident angle. An investigation into the relationship between the resolutions obtained with LSAR and CSAR or in other words the investigation into the enhancement of SAR spatial resolution with CSAR is necessary.

In this paper, a comparison between the spatial resolutions obtained with LSAR and CSAR in theory and in empirical scenario is presented. Presently, there are not many available SAR systems synthesizing circular apertures (CSAR). Few systems are available like CARABAS [7] which are mainly exploited by the defence agencies and thus SAR data becomes difficult to access. Some CSAR data sets like GOTCHA [8] are available but it is not allowed to mail these data sets out of the country of origin. The comparison between the spatial resolutions obtained with LSAR and CSAR in practice will therefore be relied on the experimental ground-based SAR system of Blekinge Institute of Technology (BTH GB-SAR) [9]. The GB-SAR

*These authors contributed equally to this work.

D. N. Nehru, V. T. Vu and M. I. Pettersson are with the Department of Electrical Engineering, Blekinge Institute of Technology, Karlskrona, 37143 Sweden e-mail:dheeraj.nehru@stud.bth.se, viet.thuy.vu@bth.se

The manuscript is submitted for publication in RADARCON 2014, Cincinnati, OH, May 2014.

system is quite helpful to carry out research which restrains the unmanageable expenses that arise of carrying out measurement campaigns.

The rest of this paper is organized as follows. Section II presents an investigation into the spatial resolutions obtained with LSAR and CSAR in theory. An investigation into the spatial resolutions obtained with LSAR and CSAR in an empirical scenario is given in Section III. Also in this section, utilizing the BTH GB-SAR system for this investigation and the proposed radar reflector for measurements with circular apertures are presented in detail. The important findings of the study are summarized in the Section IV.

## II. LSAR AND CSAR RESOLUTION IN THEORY

In this section, an investigation into the spatial resolutions obtained with LSAR and CSAR in theory will be presented. The resolutions equations for LSAR and CSAR are therefore utilized for analysis. The verification of the analysis is based on simulated LSAR and CSAR data.

### *A. LSAR and CSAR resolution equations*

For a LSAR system, the common assessments for resolution are azimuth and range resolutions. The former corresponds to the motion of the platform whereas the later is associated with radar range. In [5], the azimuth resolution in a general case is defined by

$$\Delta_{\rho_x} = \epsilon_x \frac{0.2211\lambda_c}{\sin\left(\frac{\phi_0}{2}\right)} \tag{1}$$

where $\lambda_c$ is the wavelength of center frequency and $\phi_0$ is the effective integration angle, and $\epsilon_x$ is a factor showing the azimuth/range coupling. This factor appears mainly in ultrawideband and ultrawidebeam systems whose azimuth/range coupling is serious. For narrowband and narrowbeam system, this factor can be approximated by one. Equation (1) is therefore simplified to

$$\Delta_{\rho_x} = \frac{\lambda_c}{4\sin\left(\frac{\phi_0}{2}\right)} \tag{2}$$

or even

$$\Delta_{\rho_x} = \frac{\lambda_c}{2\phi_0} \tag{3}$$

for very small effective integration angle. From the azimuth equations, it could be understood that azimuth resolution can be enhanced with the use of higher center frequency and/or higher effective integration angle.

The range resolution equation is derived in [5] as a function of radar signal bandwidth $B$ and given by

$$\Delta_{\rho_y} = \epsilon_y \frac{0.4422\mathrm{c}}{B} \tag{4}$$

where c represents the speed of propagation and is equal to that of light. The azimuth/range coupling factor $\epsilon_y$ in (4) has similar physical meaning of the one given in (1). However, the behavior of $\epsilon_x$ and $\epsilon_y$ with respect to the fractional bandwidth (ratio of bandwidth to center frequency) and effective integration angle is different. In narrowband and narrowbeam cases, the following approximation is valid

$$\Delta_{\rho_y} = \frac{\mathrm{c}}{2B} \tag{5}$$

The range resolution equations imply that the wider bandwidth a LSAR system has, the better range resolution that system can be achieved.

For a LSAR system, the same azimuth and range resolutions are obtained when

$$\phi_0 = 2\mathrm{acrsin}\left(\frac{\epsilon_x}{\epsilon_y}\frac{B_r}{2}\right) \approx 2\mathrm{acrsin}\left(\frac{B_r}{2}\right) \tag{6}$$

where $B_r$ denotes fractional bandwidth.

For a CSAR system, since the trajectory of SAR platform is circular path, azimuth and range directions do not exist and thus there is only one unique spatial resolution which depends strongly upon the bandwidth. In [6], this dependence is represented by

$$\Delta_{\rho_r} = \epsilon_r \frac{0.4422\mathrm{c}}{B} \tag{7}$$

where $\epsilon_r$ is the broadening/narrowing factor which is show to be a function of incident angle and fractional bandwidth.

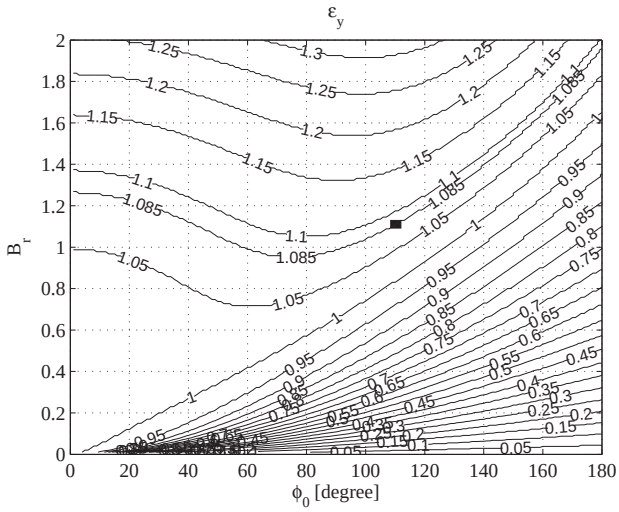


Fig. 1. Azimuth/range coupling factor $\epsilon_y$.

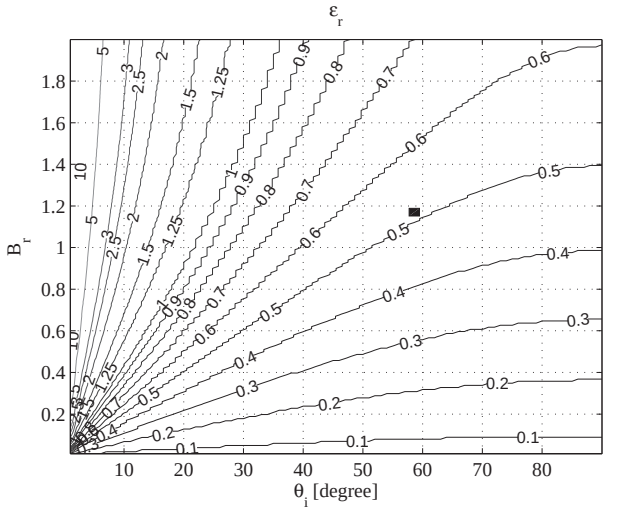


Fig. 2. Broadening/narrowing factor $\epsilon_r$.

### *B. Analysis*

The investigation into the theoretical LSAR and CSAR resolutions in this paper is limited by range resolution for LSAR and spatial resolution for CSAR. Azimuth resolution is assumed to be equal to range resolution for LSAR. Thus, if we compare (4) and (7), we can see that the difference between the range resolution of a LSAR system and spatial resolution of a CSAR system is decided by the azimuth/range coupling factor $\epsilon_y$ and the broadening/narrowing factor $\epsilon_r$. Fig. 1 and Fig. 2 show the behavior of these factors with respect to fractional bandwidth and integration angle or incident angle.

As observed in Fig. 1 and Fig. 2, for SAR systems with conventional parameters, CSAR system results in much better resolution than LSAR systems. For example, for CARABAS with the fractional bandwidth of about 1.16, the integration angle of $110^o$, and the incident angle of $58^o$ (marked by the solid black rectangles in Fig. 1 and Fig. 2), the factors are approximately 1.085 for LSAR and 0.5 for CSAR. This means the resolution can be enhanced more than two times if CARABAS synthesizes a circular aperture instead of a linear aperture.

However, if we only the increase integration angle and keep the fractional bandwidth low for a LSAR system (lower right corner of Fig. 1), the coupling factor can be reduced significantly, i.e. the SAR resolution is enhanced. It should be observed that even though this change reduces the coupling factor, such case can lead to narrow bandwidth signal which again may not enhance the resolution because of the presence of signal bandwidth in the denominator of range resolution equation (3). The same effect can be obtained with a CSAR system by increase in incident angle and decrease in fractional bandwidth (lower right corner of Fig. 2). In these cases, the enhancement in resolution of CSAR is not significantly in comparison to LSAR. It should be noticed that for high incident angles, either the radius of circular aperture may be too large or the altitude of the radar platform may be too low.

TABLE I
PARAMETERS FOR LSAR AND CSAR SIMULATIONS.

| Parameter | LSAR | CSAR |
|---|---|---|
| The highest processing frequency | 2.5 GHz | 2.5 GHz |
| The lowest processing frequency | 1.5 GHz | 1.5 GHz |
| Altitude of the ground-based SAR system | 1.25 m | 1.25 m |
| Minimum range | 2.86 m | 2.86 m |
| Aperture step | 0.05 m | 0.10 m |
| Synthetic aperture length | 1.2 m | 16 m |
| Number of aperture positions | 25 | 150 |

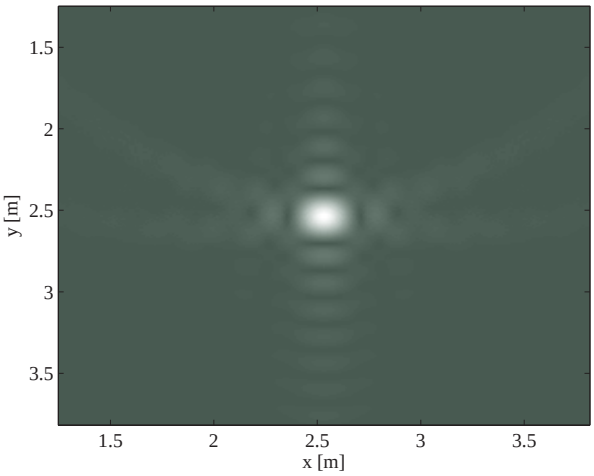


Fig. 3. SAR image formed with simulated LSAR data.

In contrary, if we only the increase fractional bandwidth and keep the integration angle low for a LSAR system (upper left corner of Fig. 1), this will not help to enhance the range resolution. The resolution will be degraded (up to $30\%$) if the LSAR system utilizes too high fraction bandwidth and too low integration angle. The same situation happens for a CSAR system with high fractional bandwidth and low incident angle (upper left corner of Fig. 2). However, the degradation in this case is extremely serious (even more than 10 times).

### *C. LSAR and CSAR simulations*

In this subsection, we present some simulation results for illustrating the analysis in the previous subsection. We select randomly a set of SAR parameters to simulate a LSAR system and a CSAR system illuminating a ground scene. The SAR scene includes only a single point-like scatterer located in the middle of the scene. The simulated data is exploited to reconstruct the SAR scene. The resolutions of the SAR images are measured and evaluated. For convenience, we select the parameters of the BTH GB-SAR system and these parameters are summarized in Table I.

For the LSAR simulation, the azimuth and range resolutions are expected to be the same due to the limitation of the investigations. The integration angle being synthesized by the system is therefore estimated from (6) with the consideration of the coupling and broadening/narrowing factors. The estimation gives the integration angle of $48^{\,\mathrm{o}}$. Using the condition for aperture step size derived in [9], we can show the aperture step size to be 0.05 m. In the LSAR simulation, the spotlight mode is considered. In this mode, the antenna is rotated in order to keep itself in a direct contact with the scatterer during movement of the antenna. In other words, the antenna is always in contact with the scatterer through its mainlobe. This results in a swath only on the SAR scene during the entire path of motion. Fig. 3 shows the SAR image reconstructed with the simulated data using the Global Backprojection (GBP) algorithm [10]. As shown, the point-like scatterer is well focused and appears as a point target. The characteristics of wide signal bandwidth and wide integration angle can be clearly observed from Fig. 3 (non- and orthogonal sidelobes).

For the CSAR simulation, we use the same parameters. The incident angle is easily calculated as $64^{\mathrm{o}}$ by applying trigonometric function for the altitude and the minimum range. If we use the same aperture step size, i.e. 0.05 m, the number of aperture positions will be 320, i.e. more than 12 times number of aperture positions in the LSAR case. The aperture length is up to 16 m. If we use the same number aperture positions, i.e. 25, the aperture step increases to 0.64 m. Our other simulations

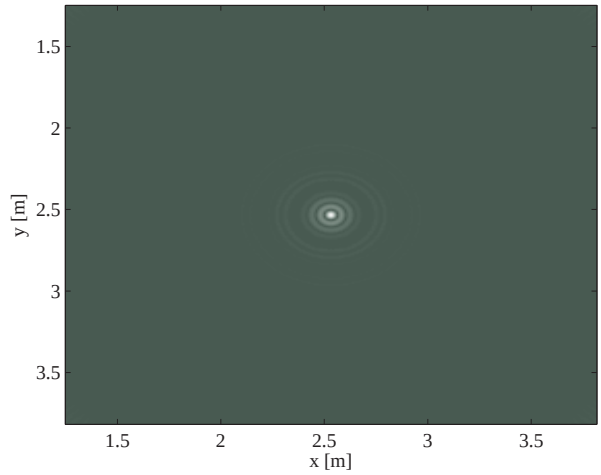


Fig. 4. SAR image formed with simulated CSAR data.

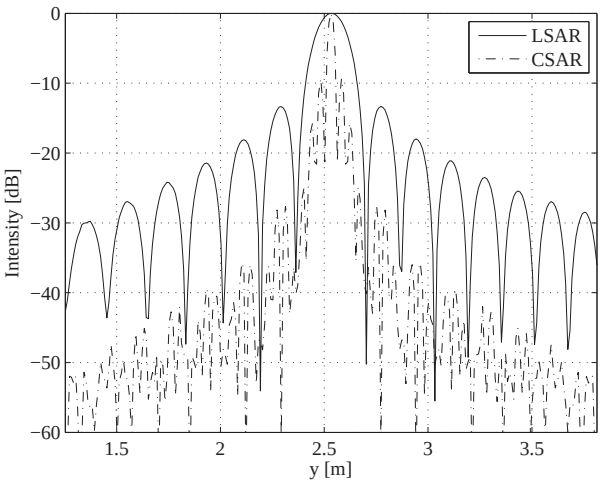


Fig. 5. Vectors extracted from images formed with simulated data in $y$ direction.

show that the aperture step does not affect the spatial resolution of CSAR. The major effect caused by big aperture steps, i.e. unwanted high sidelobe level, does not appear if we double the aperture step, i.e. 0.1 m. The number of aperture positions is therefore increased to 150. The SAR image formed with these calculated values is given in Fig. 4. One can see directly that the resolution of the image formed with the CSAR data is enhanced significantly in comparison to the one formed with the LSAR data given in Fig. 3. For a better evaluation of this enhancement, the vectors in the y direction are extracted and then the resolution measurements are performed on these vectors. The extracted vectors are plotted in Fig. 5 showing again the enhancement in resolution of CSAR. In Table II, we provide the values of resolution measured on the extracted vectors which are quite matched with the values estimated with the resolution equations. The results indicate that the circular aperture offers a much better resolution in comparison to the linear aperture. The improvement in resolution with CSAR in this case can be expressed by a factor of about 5.

## III. LSAR AND CSAR RESOLUTION IN EMPIRICAL SCENARIO

Spatial resolution enhanced with CSAR in an empirical scenario will be investigated in this section. The investigation is relied on the BTH GB-SAR system. The LSAR and CSAR data is acquired with this system and then processed according to the investigation purposes.

### *A. BTH GB-SAR and radar reflector*

BTH GB-SAR is a flexible ground-based system [9]. The flexibility is found from the wide operating frequency range of the system, the unlimited length of the synthetic aperture, the features of the synthetic aperture, e.g. linear and circular, and

TABLE II
MEASUREMENT RESULTS.

| Parameter | LSAR | CSAR |
|---|---|---|
| Resolution in theory | ≈0.14 m | ≈0.03 m |
| Resolution in empirical scenario | ≈0.15 m | ≈0.03 m |

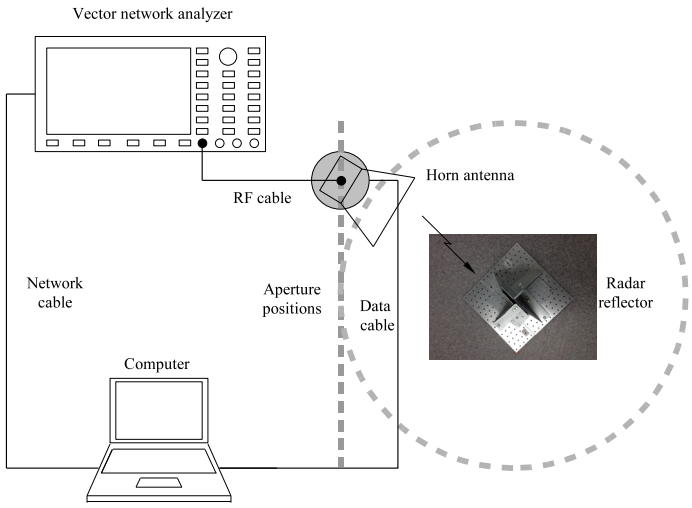


Fig. 6. BTH GB-SAR system diagram.

different acquisition modes of the system, e.g. stripmap and spotlight.

Fig. 6 shows the diagram of this system. The main components of the system include a vector network analyzer, a double ridge guide horn antenna, a computer, cables, antenna positioning, and other accessories.

It is common knowledge that a normal dihedral corner reflector can only reflect incident wave from certain directions and therefore not appropriate for measurements with a circular aperture. We propose to use a special radar reflector having diamond shape in the following experiments. The structure of this radar reflector allows reflecting incident wave from any direction. The maximum dimension of the radar reflector is about 50 cm. Although the dimension of the radar reflector is not optimum for the selected frequency range its reflection is still significant.

### *B. Experiments*

The BTH GB-SAR system is configured according to the parameters given in Table I. The SAR scene is the radio communication laboratory of BTH. The diamond shaped radar reflector is located in the center of the SAR scene.

The operation mode of the system in data acquisition is spotlight. This mode of operation helps during the experimentation in an environment like laboratory to obtain a maximum reflection from the reflector which otherwise contains reflections from other apparatus in the laboratory.

The system will collect the data for the LSAR and CSAR cases. Again, all the parameters used of LSAR are same to that of CSAR apart from the aperture steps and the numbers of aperture positions. The aperture steps and the numbers of aperture positions are identical to the ones which have been used for the LSAR and CSAR simulations. The procedure of data acquisition is vividly portrayed in the [9]. It should be noticed that we should use a small window for the gating function in the vector network analyzer to suppress as much as possible the reflections from other apparatus in the laboratory, especially in the CSAR case where the radar range with respect to the radar reflector is constant.

### *C. Measurements*

The LSAR and CSAR data are used to reconstruct the SAR scene using the GBP algorithm. Fig. 7 and Fig. 8 provide the images of the SAR scene illuminated by the GB-SAR system synthesizing linear and circular aperture, respectively. The radar reflector appears in Fig. 7 as a point-like scatterer whereas the detail of the radar reflector can be observed in Fig. 8. The structure of the radar reflector given in the SAR image in Fig. 8 is similar to the structure in reality which can see from Fig. 6. This due to the significant improvement in resolution of the CSAR case.

Fig. 9 shows the vectors extracted from Fig. 7 and Fig. 8 in the y direction for resolution measurements. The measurement results given in Table II indicate that the resolutions in theory and in the empirical scenario are almost identical. In other

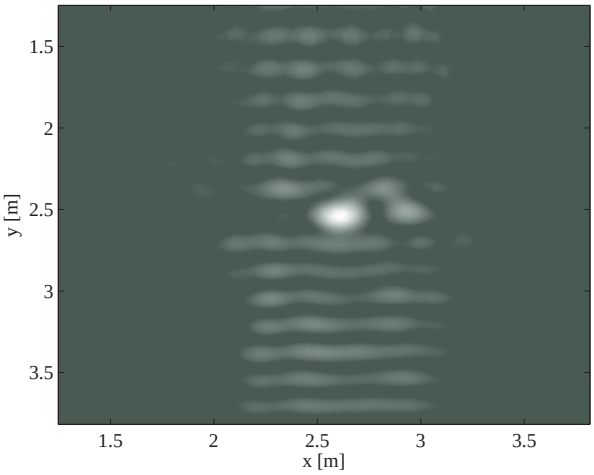


Fig. 7. SAR image formed with real LSAR data.

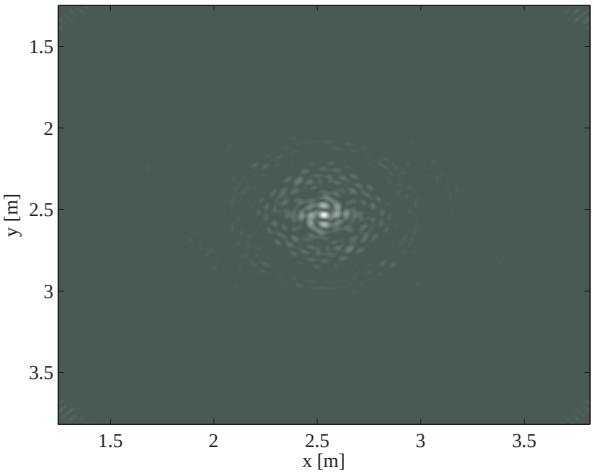


Fig. 8. SAR image formed with real CSAR data.

words, the enhancement in resolution of CSAR in practice is similar to that in theory. The improvement in resolution with CSAR in this case can also be expressed by a factor of about 5.

## IV. Conclusion

This paper deals with the strategy to increase resolution of SAR image with circular aperture. The effects with the use of circular aperture are vividly explained by the theoretical analysis followed by the simulated results and the practical observations. In order to restrain from the unmanageable expenses of carrying out field campaigns, the empirical data is obtained with the BTH GB-SAR system. The unique structure of the radar reflector has been used to achieve prominent reflections while collecting the practical data using linear and circular apertures. The enhancement of resolution is evident from the results obtained and the resolution achieved by CSAR is around 5 times better than that of LSAR ones with the chosen parameter set. However, there is a mismatch between the theoretical and practical results which could be an effect due to prorogation loses or caused by the laboratory environment.

## Acknowledgment

The authors would like to thank the KK-Foundation for making this research project possible, and are also appreciative of support from the Swedish Defence Research Agency, Saab Bofors Dynamics, Saab Microwave Systems and RUAG Space.

$$\Lambda = \frac{\epsilon_r}{\epsilon_y} \tag{8}$$

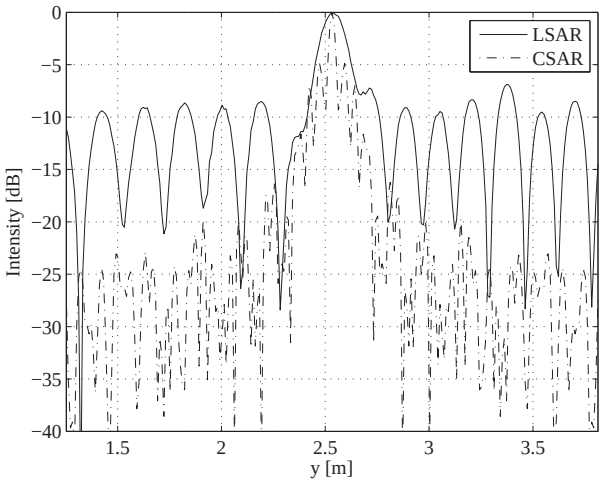


Fig. 9. Vectors extracted from images formed with real data in $y$ direction.

## REFERENCES

[1] P. Patel, H. S. Srivastava and R. R. Navalgund, "Use of synthetic aperture radar polarimetry to characterize wetland targets of Keoladeo national park, Bharatpur, India", *Current Science*, vol. 97, no. 4, pp. 529–537, 2009.

[2] N. Casagli, P. Farina, D. Leva, G. Nico and D. Tarchi, "Monitoring the Tessina landslide by a ground-based SAR interferometer and assessment of the system accuracy", in *Proc. IEEE IGARSS'2002*, vol. 5, Toronto, Canada, Jul. 2002, pp. 2915–2917.

[3] K. Leilei, W. Xiaoqing, Z. Minhui, C. Jinsong and X. Maosheng, "Resolution analysis of circular SAR with partial circular aperture measurements", in *EUSAR'2010*, Aachen, Germany, pp. 1–4, 2010.

[4] R. Sharma, "Analysis of circular aperture SAR image formation", in *Forty-Third Asilomar Conference on Signals, Systems and Computers*, Pacific Grove, CA, 2009, pp. 482–487.

[5] V. T. Vu, T. K. Sjögren and M.I. Pettersson, "On synthetic aperture radar azimuth and range resolution equations", *IEEE Trans. Aerosp. Electron. Syst.*, vol. 48, no. 2, pp. 1764–1769, 2012.

[6] V. T. Vu, T. K. Sjögren and M.I. Pettersson, "Studying CSAR systems using IRF-CSAR", in *Proc. IET RADAR*, Glasgow, UK, Oct. 2012, pp. 1–6.

[7] P.-O. Frölind, A. Gustavsson, M. Lundberg and L.M.H Ulander, "Circular-aperture VHF-band synthetic aperture radar for detection of vehicles in forest concealment," *IEEE Trans. Geosci. Remote Sensing*, vol. 50, no. 4, pp. 1329–1339, 2012.

[8] E. Ertin, C. D. Austin, S. Sharma, R. L. Moses and L. C. Potter, "GOTCHA experience report: Three-dimensional SAR imaging with complete circular apertures," *SPIE Algorithms for Synthetic Aperture Radar Imagery XIV*, vol. 6568, Orlando, FL, Apr. 2007. pp. 02–13.

[9] V. T. Vu, D. N. Nehru, T. K. Sjögren and M.I. Pettersson, "An experimental ground-based SAR system for studying SAR fundamentals", in *Proc. APSAR 2013*, Tsukuba , Japan, Sep. 2013, accepted for publication.

[10] L. E. Andersson, "On the determination of a function from spherical averages", *SIAM Journal on Mathematical Analysis*, vol. 19, no. 1, pp. 214–232, 1988.

# Experimental Results on the Ground Based SAR System Images for Different Aperture Parameters and Modes of Operation.

Dheeraj Nehru Neravati

June 2013

# Abstract

In the paper published in [1], the requirement of the experimental ground-based SAR (GB-SAR) system for extracting the data is explained. The procedure that is to be followed for channel measurement is also portrayed. In this report, few results obtained from the data extracted by the experimental GB-SAR system are provided to give more insight into the impacts of aperture parameters on the resolutions and the quality of the SAR image. The impact of different SAR modes of operation is also represented.

## Table of Contents

## List of Figures & Tables:

# Chapter 1
# Introduction

This chapter gives the introduction to the report. In particular the types of experiments performed are presented. Results obtained with simulation and the setup of the experimental SAR system and its initialization are presented. GBP algorithm is used for SAR scene reconstruction for simulation and all other experiments.

## 1.1 Types of Experiments

In this chapter the summary of the types of the experiments is provided. This report focuses on the changes in the quality of SAR images and the resolutions with different aperture parameters and modes of operation.

Experiments based on linear aperture (LSAR):
With 17 aperture points for spotlight mode
With 71 aperture points for spotlight mode (with and without matched filtering)
With 71 apertures for stripmap mode (with and without matched filtering)
Effects of having more aperture positions & need for proper aperture step
Effects of gating with narrow and wide window widths
Effects on azimuth resolution at different integration angles

Circular Aperture:
With 32 apertures and 64 aperture positions for spotlight mode without matched filtering
With span corresponding to total SAR scene image and span corresponding to only the reflection from target reflector.

## 1.2 Simulation

The simulated results are shown for initial understanding and then followed by the results obtained from the experiments. In the first step, SAR system is simulated by modelling the path of synthetic aperture. In the second step, channel is modelled to achieve SAR raw data. In the third step, pulse compression is carried out. In the fourth step, image

scene is constructed with the GBP algorithm. MATLAB is used as the tool for simulating the SAR system.

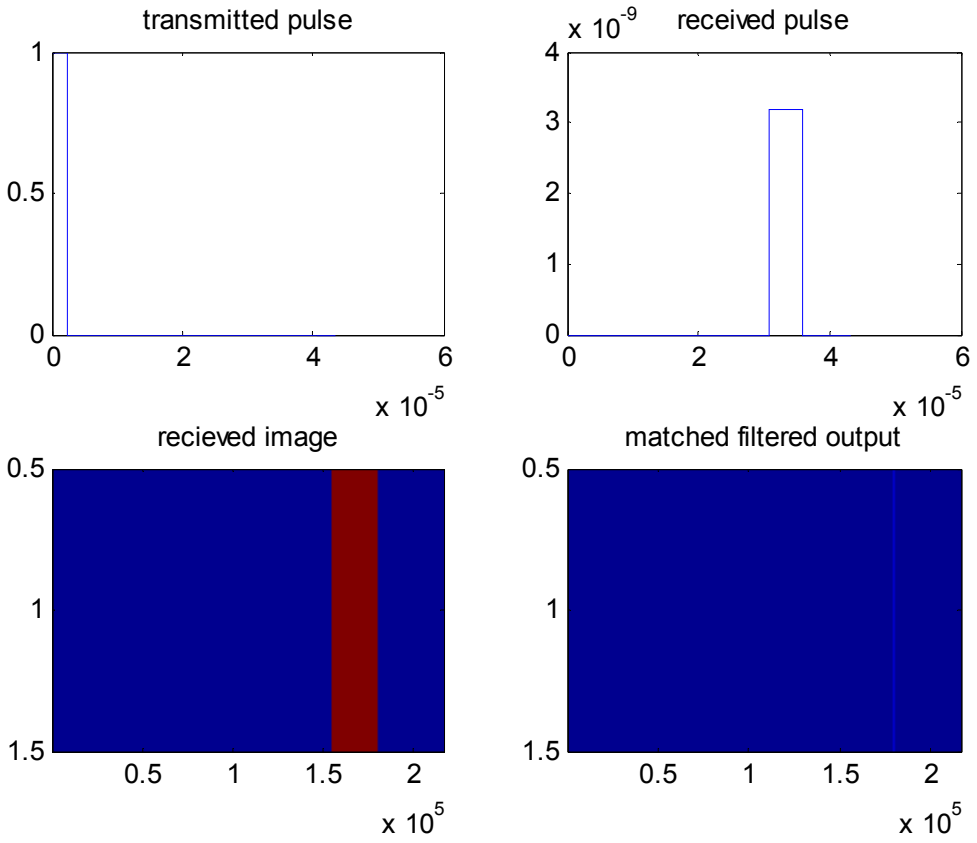


Figure 1: transmitted pulse, received pulse, received image and matched filtered

The plot in Fig.1 represents the importance of pulse compression. The requirement of matched filtering technique for pulse compression in order to obtain a better resolution could be understood from Fig. 1 in which pulse width of the received signal is much wide than that of the matched filter output. This is because of the fact that when the pulse compression is achieved by matched filtering, the received signal shown in Fig.1 is converted to a sinc function as shown in Fig.2.

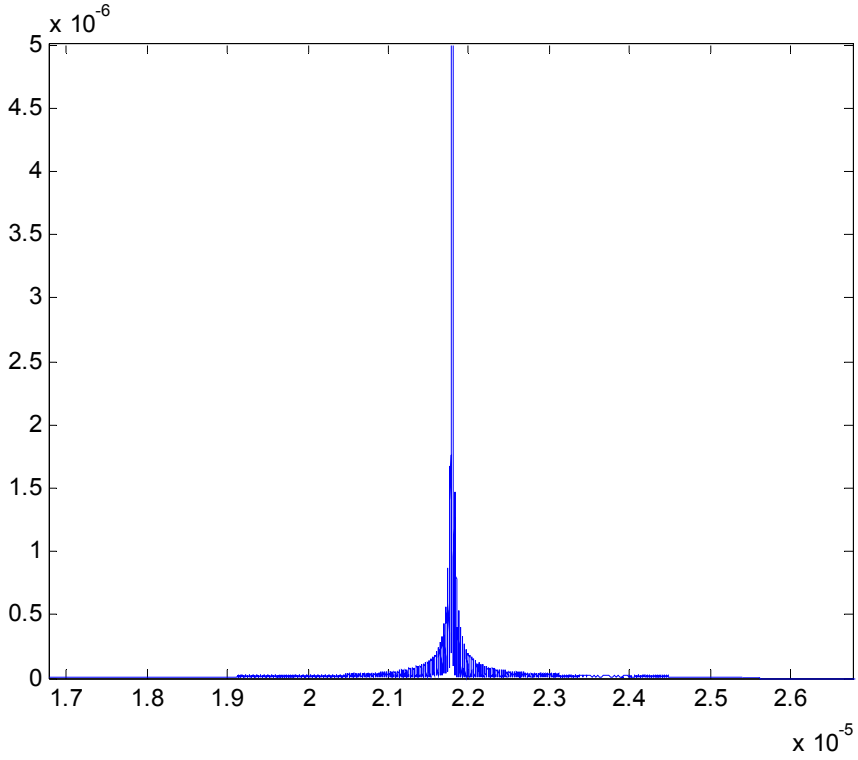


Figure 2: Pulse compressed signal representing a sinc function.

The SAR scene image formed with the data of SAR system synthesizing a linear aperture (LSAR) after pulse compression and interpolation is shown in Fig. 3. The SAR system is simulated using CARABAS parameters. In this image, the *x*-axis corresponds to the azimuth direction where as *y*-axis corresponds to the range direction.

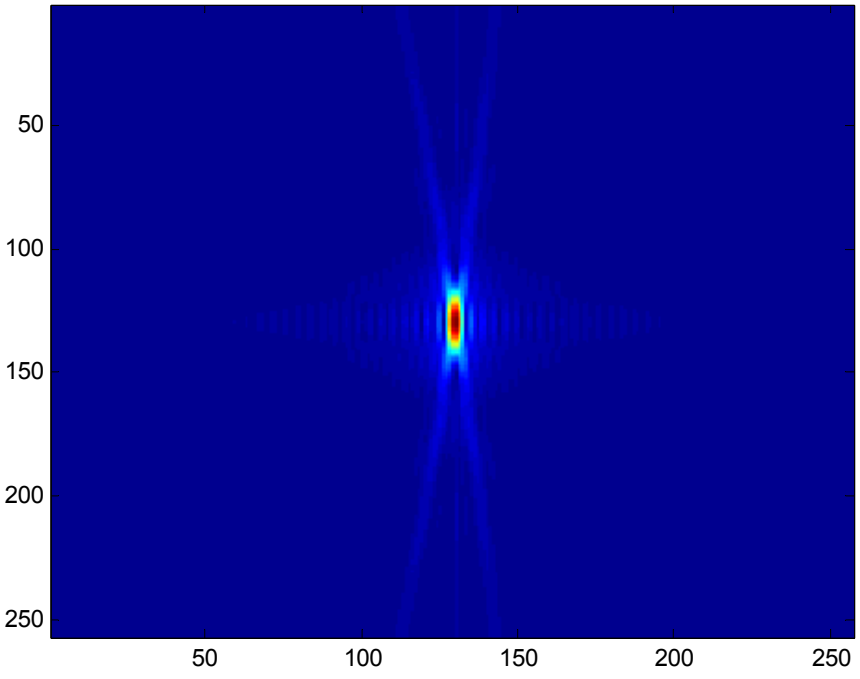


Figure 3: SAR scene image for Linear Aperture with CARABAS Parameters.

The SAR scene image formed with the data of the SAR system synthesizing a circular aperture (CSAR) after pulse compression and interpolating using the same CARABAS parameters is shown in Fig. 4.

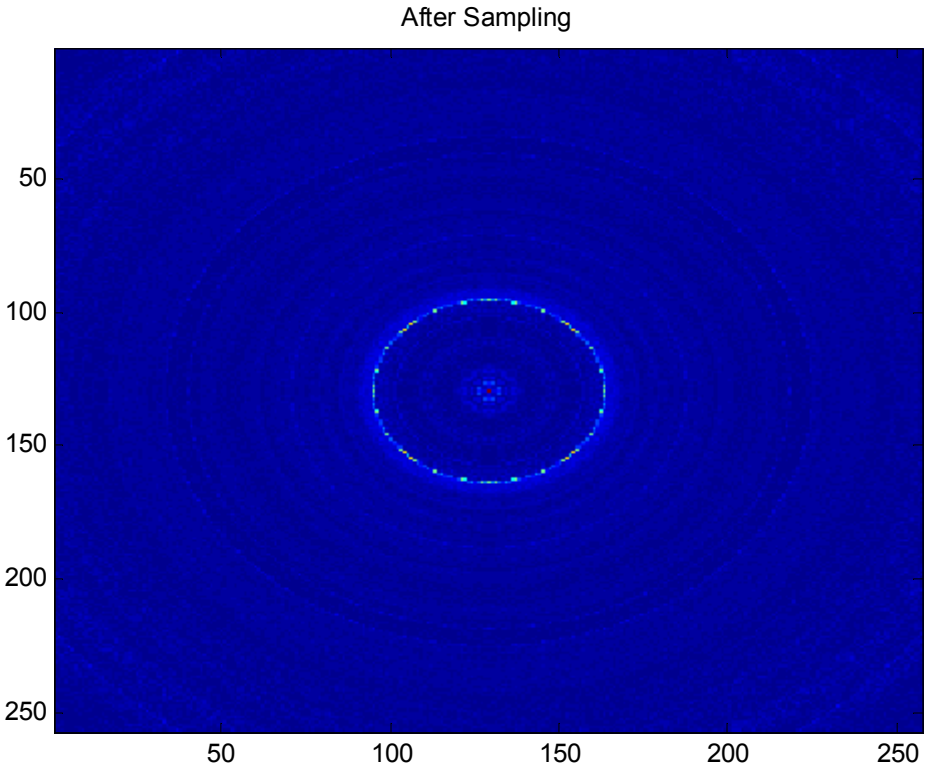


Figure 4: SAR scene image for Circular Aperture with CARABAS II Parameters.

Looking at the SAR image formed by circular aperture data after pulse compression and interpolation, it could be observed that resolution achieved by circular aperture is much better than that of linear aperture counterparts. It should be remembered that in circular aperture azimuth direction does not exist because of the circular path of SAR platform motion.

## 1.3 Experiment Setup & Initialization:

Experiments are performed on the SAR system built on a Vector Network Analyzer (VNA) Agilent E5071C operating in the frequent range between 300 kHz – 20 GHz. A single horn antenna manufactured by A.H. systems is used for both transmitting and receiving making it a monostatic system. A trihedral corner reflector is deployed in the measurements to obtain reflections for the point like scatterer. The system can be seen in Fig.5 and Fig.6 which shows the antenna connected to the network analyzer and facing the corner reflector. In Fig.5 the

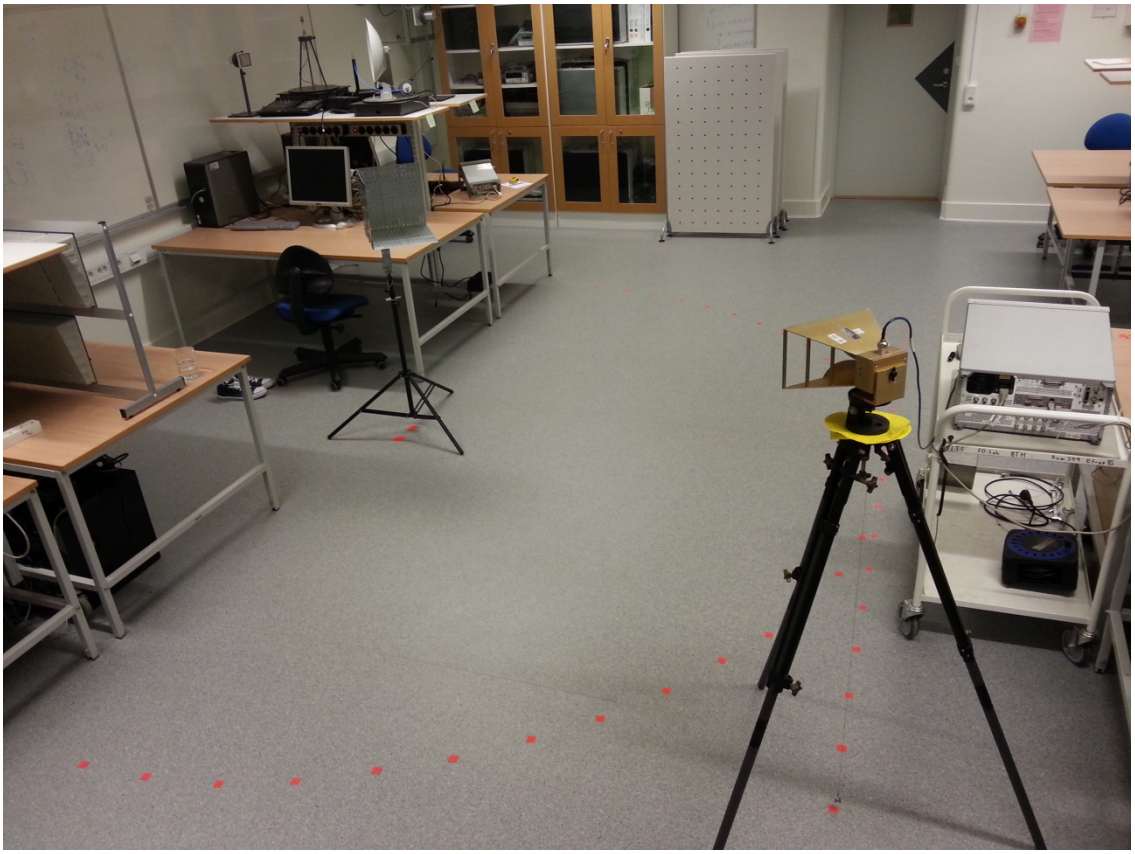

Figure 5: SAR System facing a trihedral reflector (for linear aperture).

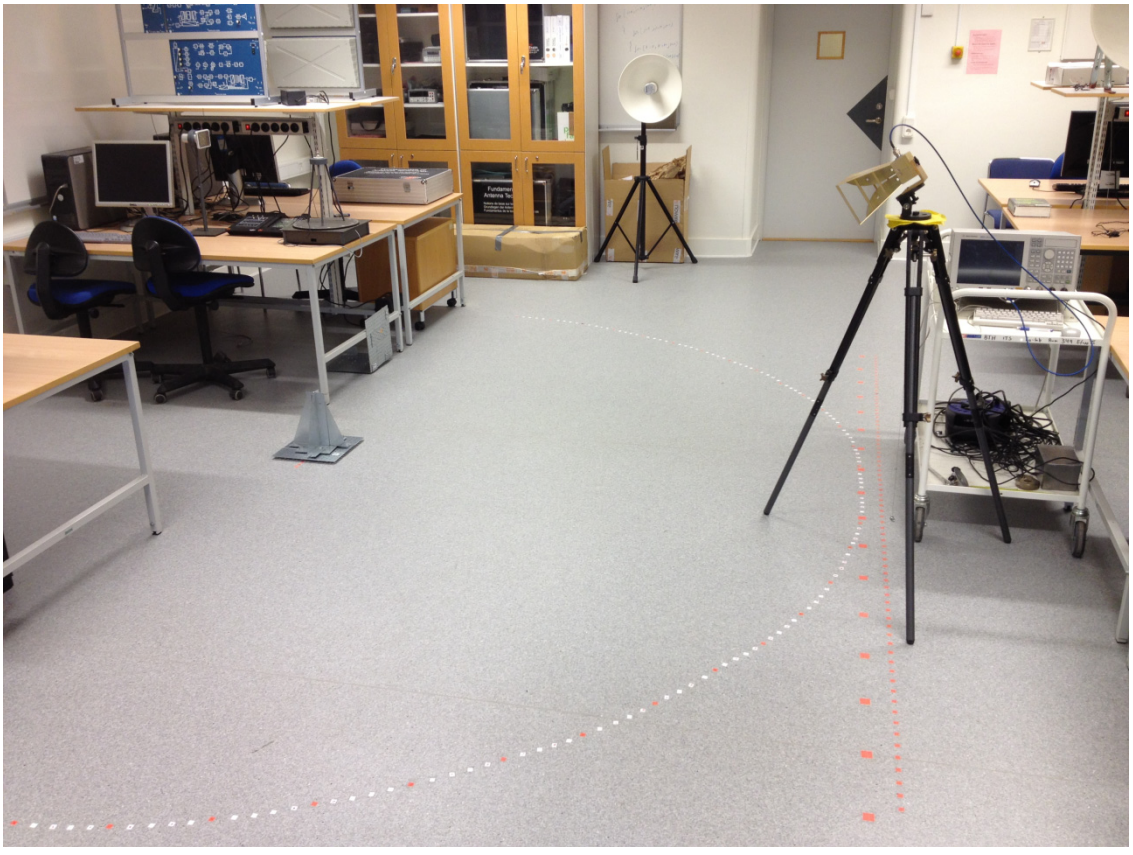

Figure 6: SAR system facing a triangular reflector (for circular aperture) showing pointed aperture positions.

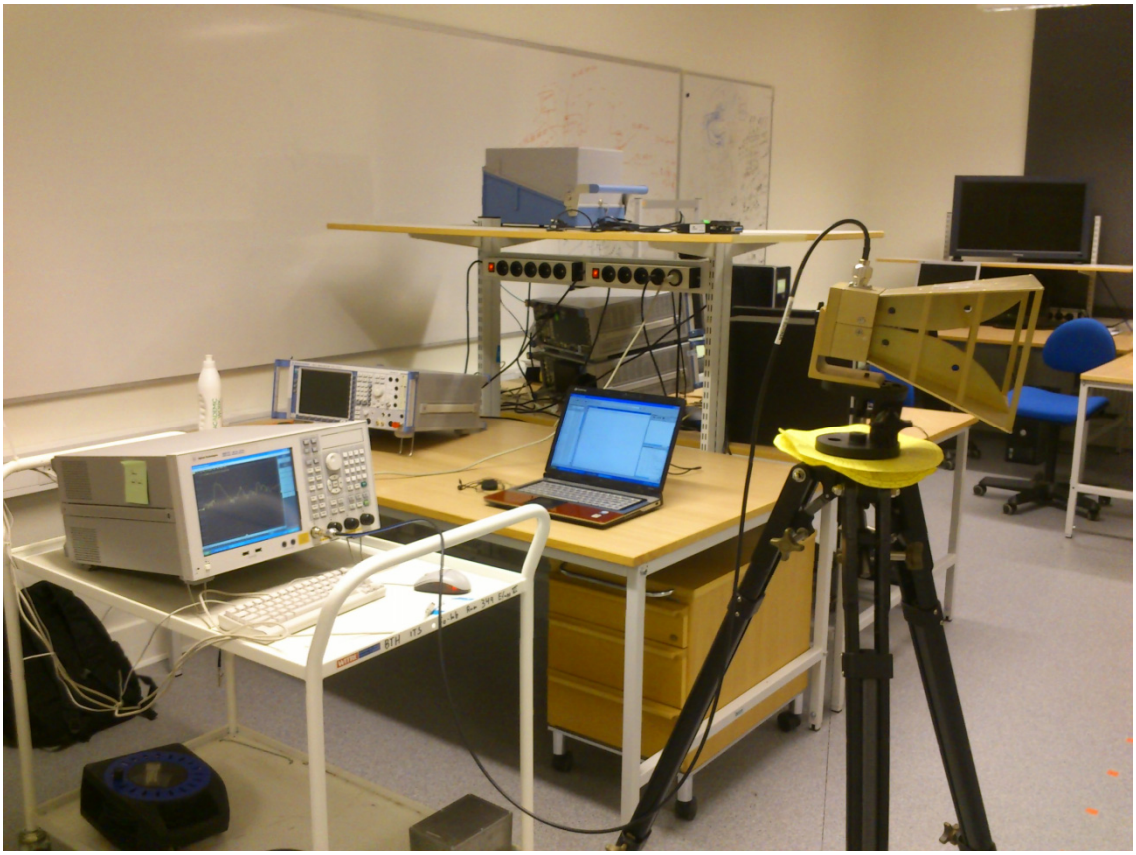

Figure 7: SAR System built on Vector Network Analyzer.

SAR system is operating for linear aperture and thus trihedral reflector is used. In Fig.6 the SAR system is operating for circular aperture and thus a triangular reflector is used which can scatter signal equally from all directions [2]. The laboratory environment can be seen which consists of many other apparatus which shall account for signal reflections as well. However the reflections from the target are stronger than from others. Both the aperture paths linear and circular are marked with red spots, due to the lack of space only a semi circle is considered with the integration angle of $180^0$. The antenna is positioned at each and every aperture and the signal is transmitted by the antenna according to the required parameters that we setup in the VNA. Data comprising of scattering parameters corresponding to the reflected signal are again received by the same antenna and then observed and stored in the VNA. A screen shot of the VNA is shown in Fig.8. The reflected signal i.e. scattering parameters can be stored in various formats as can be seen in the right side of Fig. 8 either in frequency-domain or time-domain according to our requirement or ease of signal processing. The detailed description of experimentation and signal processing can be found in [1]. The signal reconstructed on simulator (here MATLAB) from the received scattering parameters data is shown in Fig.9 and Fig.10. The plot in Fig. 9 corresponds to the frequency-domain reconstruction whereas the one in Fig. 10 correspond to its associated time-domain

reconstruction. The reconstructed signal is processed as explained before and the SAR image is obtained after applying the GBP algorithm.

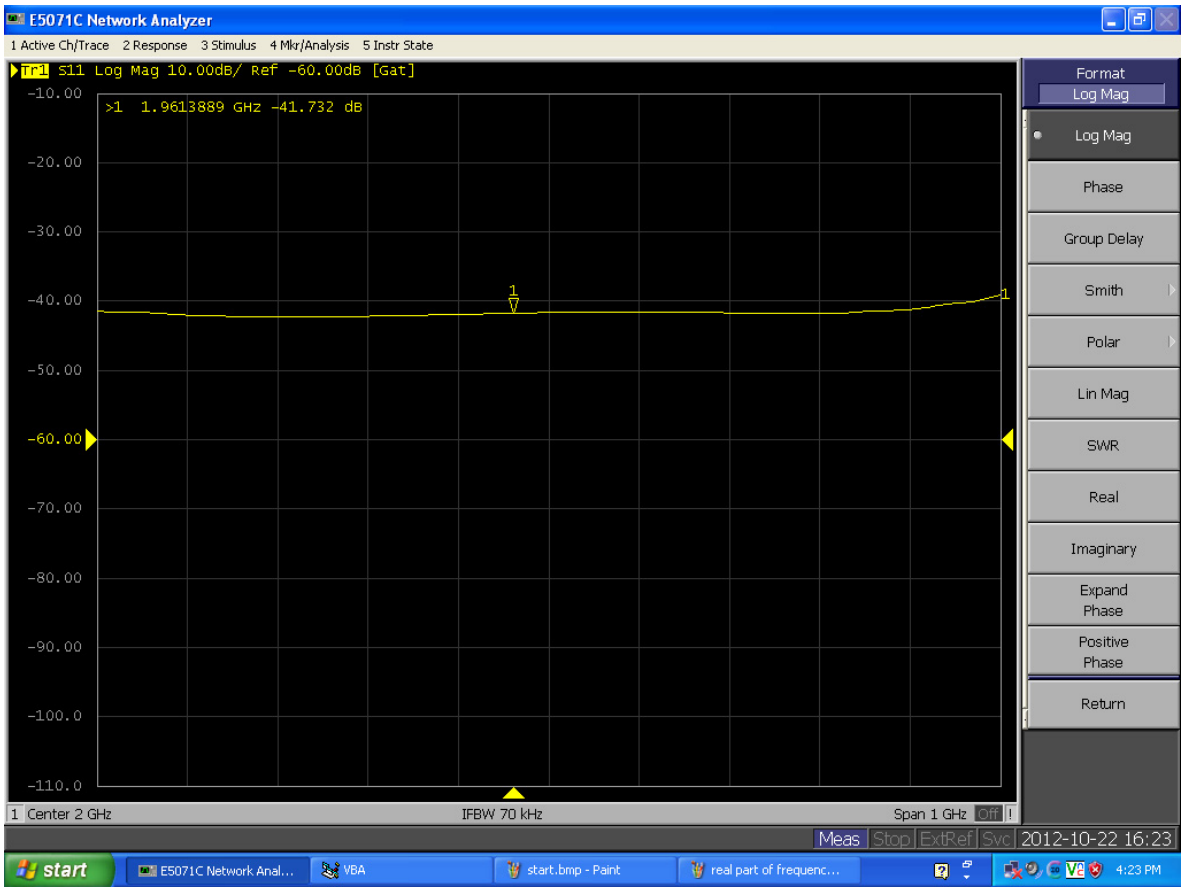


Figure 8: Screen shot of Network Analyzer screen showing the received signal in frequency domain.

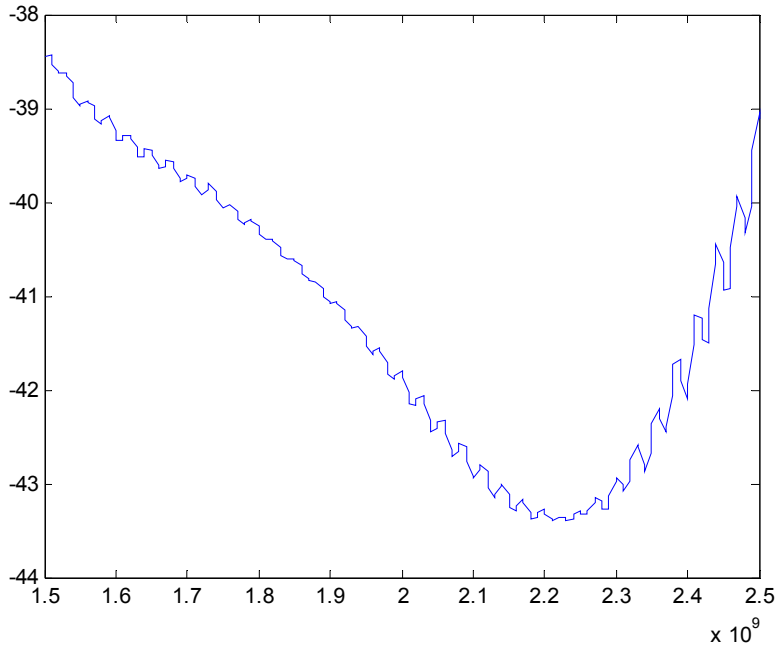


Figure 9: Image reconstructed from the data received by network analyzer in frequency domain after gating.

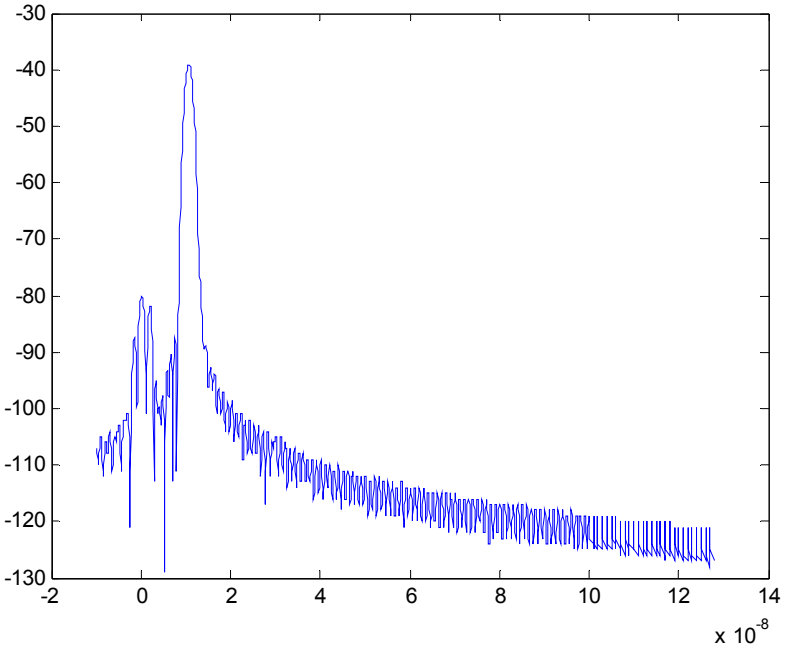


Figure 10: Image reconstructed from the data received by network analyzer in time domain after gating.

Such SAR images obtained for different kinds of experiments are described and produced in the following section for better understanding of SAR operation and its results.

In order to reconstructing the SAR image from extracted data, zero padding should be performed to fill in the unused frequencies. The plot obtained after zero padding the signal is shown in Fig. 11 with data samples on its *x*-axis and SNR on *y*-axis.

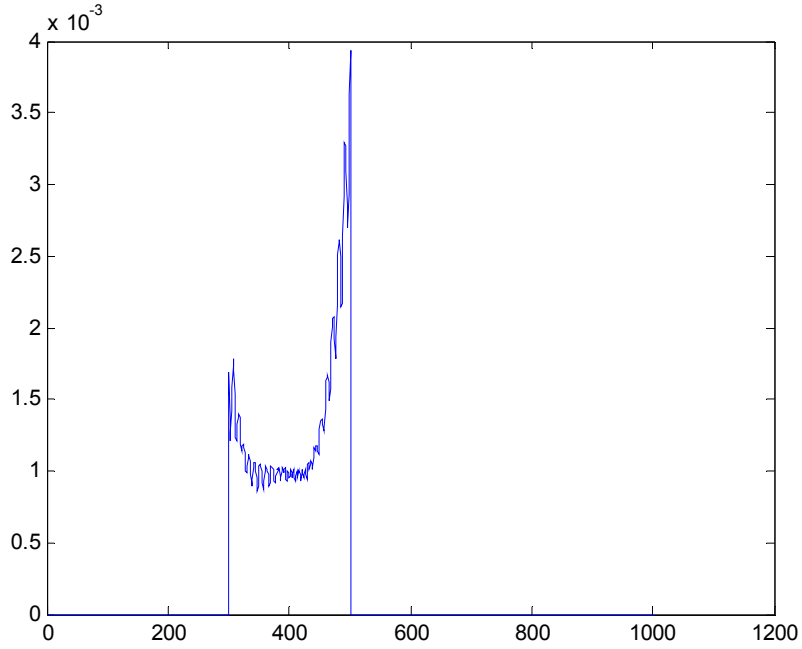


Figure 11: Image showing the signal spectrum after zero padding.

# Chapter 2

# Experiments

In this chapter results for various experiments are presented and described. The impacts of different SAR parameters and effects of SAR modes of operation are explained with results. The results presented mainly focus on the resolution and quality of SAR image. This chapter gives broad insight on the operation of SAR and its performance. In this chapter for all the linear aperture SAR images, *x*-axis represents range resolution and *y*-axis represents azimuth resolution.

## 2.1 Spotlight Mode for Linear Aperture

### *2.1.1 With 17 aperture points*

The following Fig.12 shows the SAR image scene using 17 apertures points without pulse compression but with interpolation with the up sampling rate of 2.

From the result obtained a mirror reflection of the target is visible which is an artefact caused due to change in phase of the signal. These changes in phase are observed once the radar crosses the middle aperture point which has the shortest distance to the target corner reflector. After performing the phase correction a single target is observed and can be seen in Fig. 13. The quality of the SAR image is degraded and side lobes are not clearly visible because of the selected aperture points which allow high aperture step, in this experiment aperture step is not in accordance with equation derived in [1]. Parameters used in this experiment are represented in Tab.1 and reflected signal is gated with narrow window width.

| Parameter | Setting |
|---|---|
| The highest processing frequency | 2.5 GHz |
| The lowest processing frequency | 1.5 GHz |
| Altitude of the ground-based SAR system | 1.25 m |
| Minimum range | 2.86 m |
| Aperture step | 0.24 m |
| Number of aperture positions | 17 |
| Synthetic aperture length | 3.84 m |
| Integration angle | $74^0$ |

Table 1: Parameter for experimentation with 17 apertures

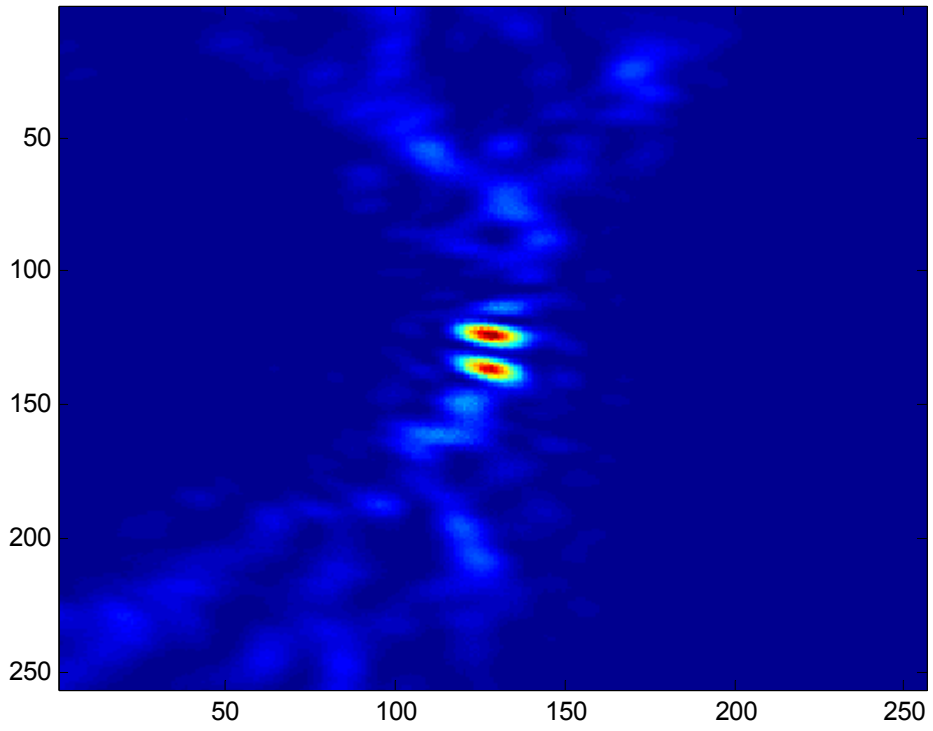


Figure 12: SAR image scene showing target deformed due to phase distortions.

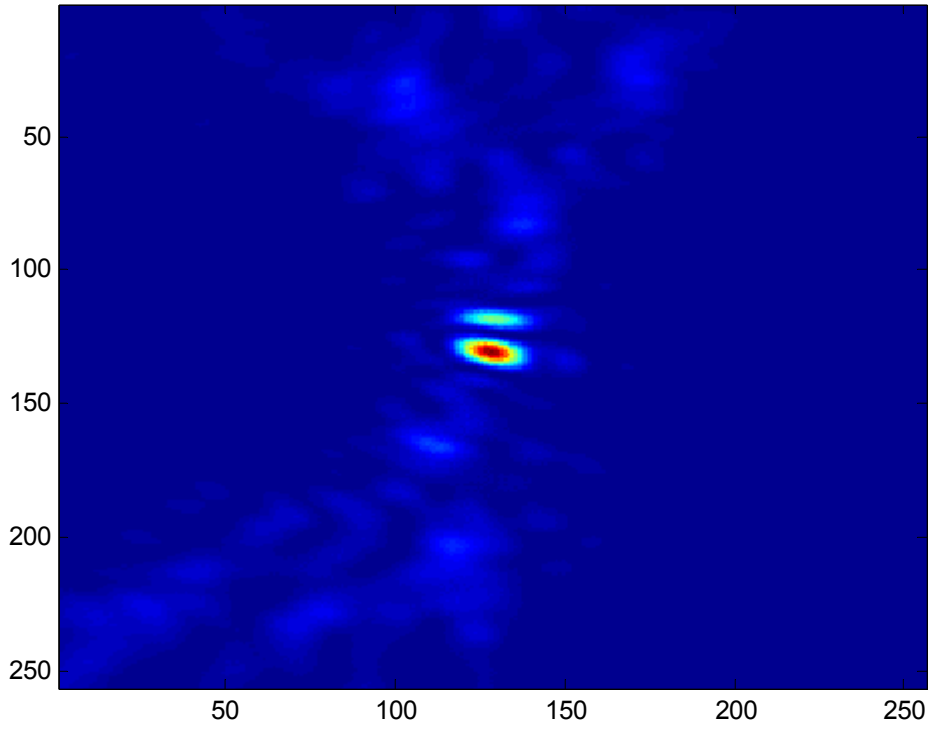


Figure 13: SAR image scene after correcting the phase distortion.

Results obtained after matched filtering show improvement in the resolution terms. When the signal is pulse compressed it shows a different trend when compared to the results without pulse compression. In without pulse compression results single target is observed after phase correction but here single target is observed before phase correction and multiple targets appear if we apply phase correction. Fig.14 shows pulse compressed SAR scene without phase correction and Fig.15 shows pulse compressed SAR scene with phase correction. Result is contrary when compared to non pulse compressed image in terms of phase correction.

Advantage of performing pulse compression technique can be clearly understood from Fig.13 and Fig.14 and thus this technique is considered as the primary method to achieve improvement in the resolution. SAR image in Fig.13 shows signal scattered away from target (light blue color spot), this effect is caused due to improper positioning of SAR antenna which in other terms called as motion error. This error could be corrected by the process of motion error compensation which is also called as autofocus correction. SAR images show considerable reflections from apparatus around the corner reflector which causes the quality of SAR image to deteriorate further. Effect of motion error is also observed in the image.

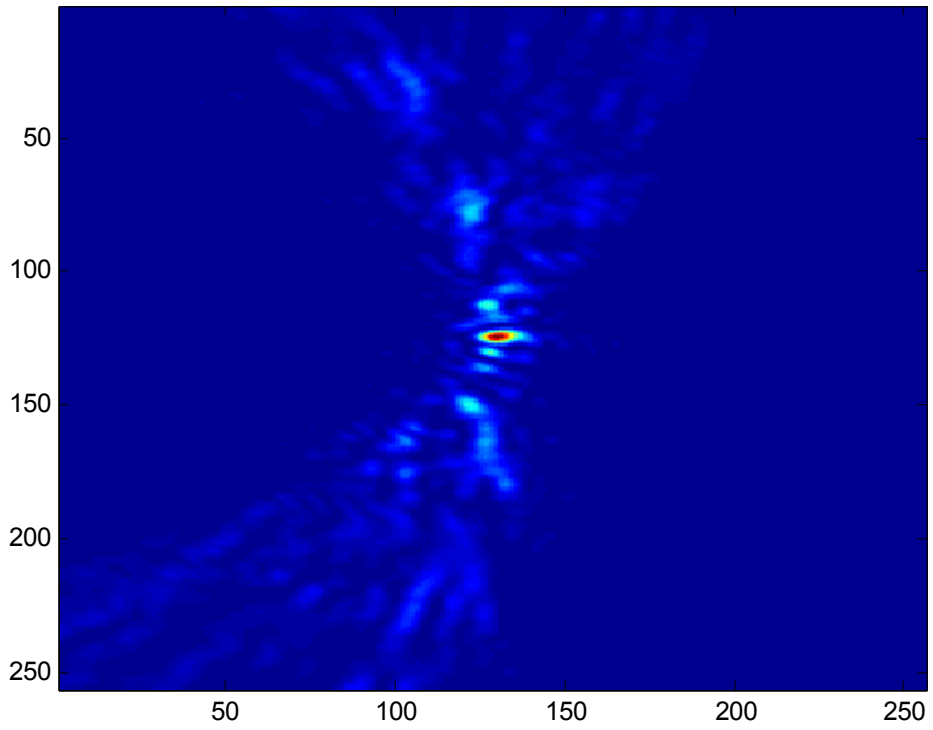


Figure 14: SAR image scene after matched filtering but without phase distortion.

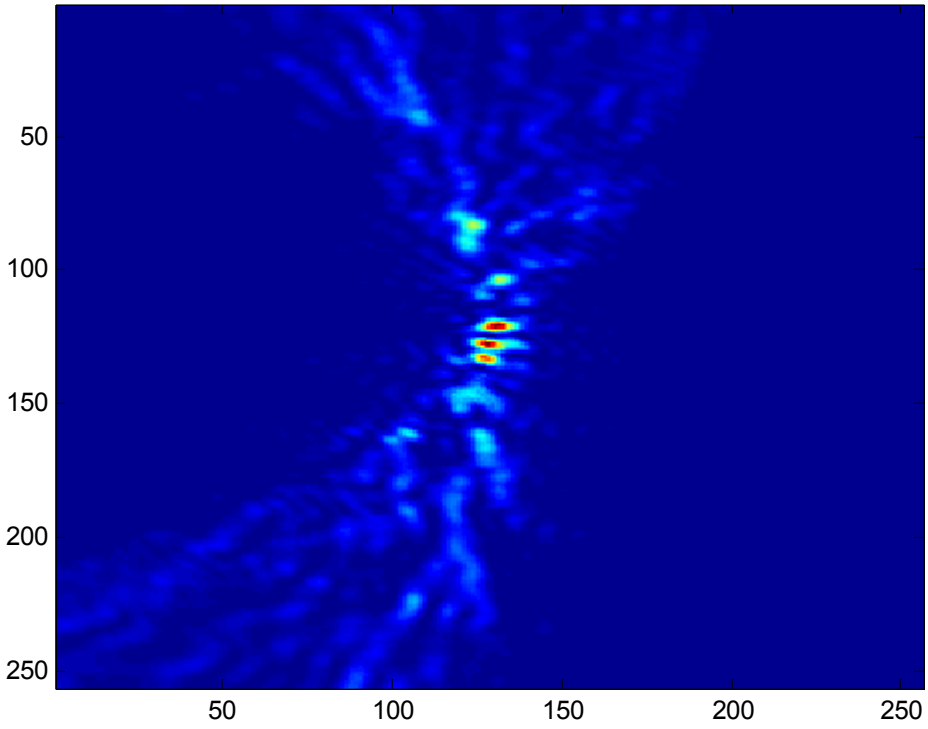


Figure 15: SAR image scene after matched filtering after applying phase correction

### 2.1.2 With 71 aperture points

Parameters used in this experiment are shown in Tab.2. Aperture step used in this experiment is in accordance with the derived equation in [1] due to which the number of aperture points raises to 71.

| Parameter | Setting |
|---|---|
| The highest processing frequency | 2.5 GHz |
| The lowest processing frequency | 1.5 GHz |
| Altitude of the ground-based SAR system | 1.25 m |
| Minimum range | 2.86 m |
| Aperture step | 0.05 m |
| Number of aperture positions | 71 |
| Synthetic aperture length | 3.50 m |
| Integration angle | $72^0$ |

Table 2: Parameters for experimentation with 71 apertures

RAW data matrix of the spotlight mode is represented in Fig.16 which looks like a perfect curve unlike stripmap mode, this is because the antenna always faces the target reflector at all the aperture positions there by attaining stronger reflections from it alone. In Fig.16 the plot shows range samples on *x*-axis and aperture position on *y*-axis. From the figure it can be understood that the maximum range to the target is from the first and last aperture positions and the range is minimum from the middle aperture position for a linear aperture.

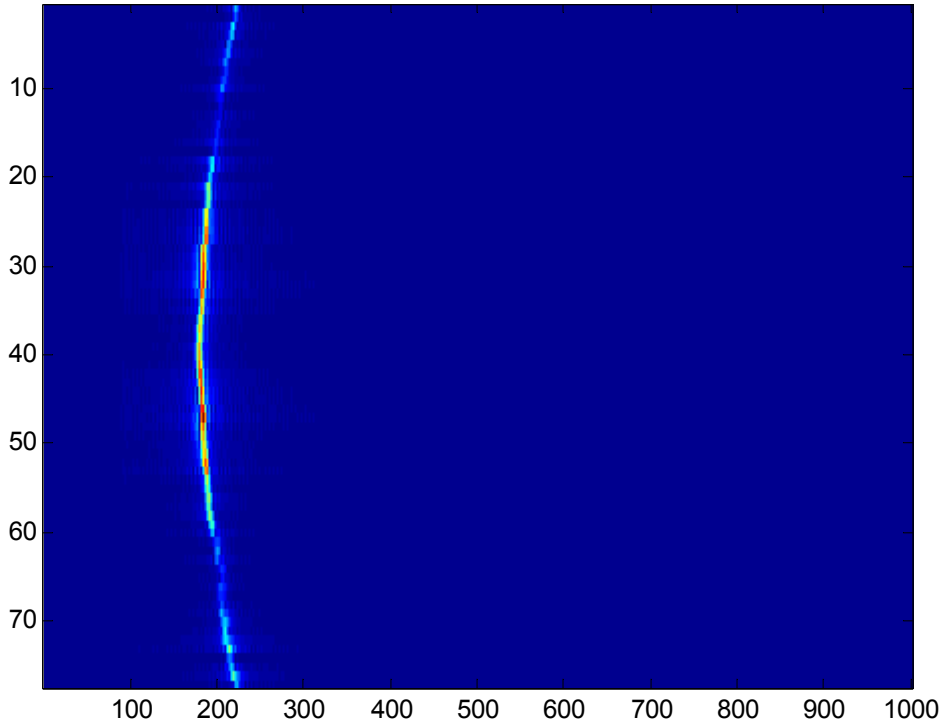


Figure 16: SAR raw data matrix for spotlight mode.

An expression for acceptable number of apertures is derived in [1] according to which 71 is the number of apertures acceptable for the parameters used. From the results obtained for 71 apertures the validity of the expression is supported. From Fig.17 the orthogonal side lobes as well as non-orthogonal side lobes of the signal are clearly visible which can't be observed in the results obtained with 17 apertures. This effect may be neglected during research with point target but it gives adverse effects in real time. Thus with the obtained results the expression derived in [1] is validated. Results shown in Fig.17 correspond to non pulse compressed image with interpolation by up sampling rate of 10 where as in Fig.18 result obtained by pulse compression technique is shown which is interpolated at an up sampling rate of 10.

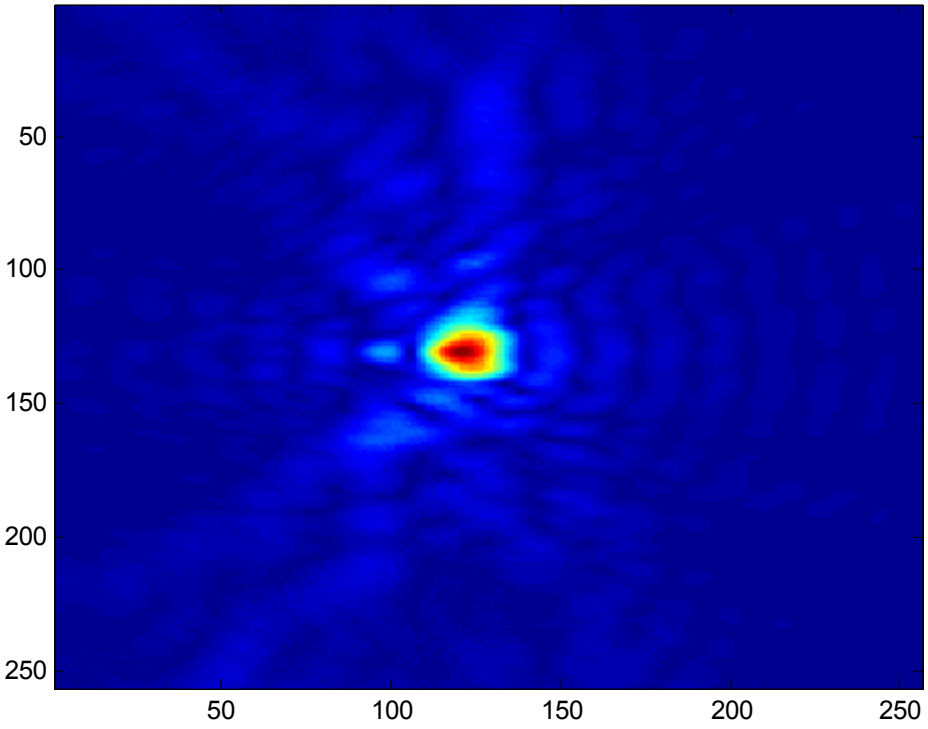


Figure 17: SAR image before pulse compression for spotlight mode with 71 aperture positions.

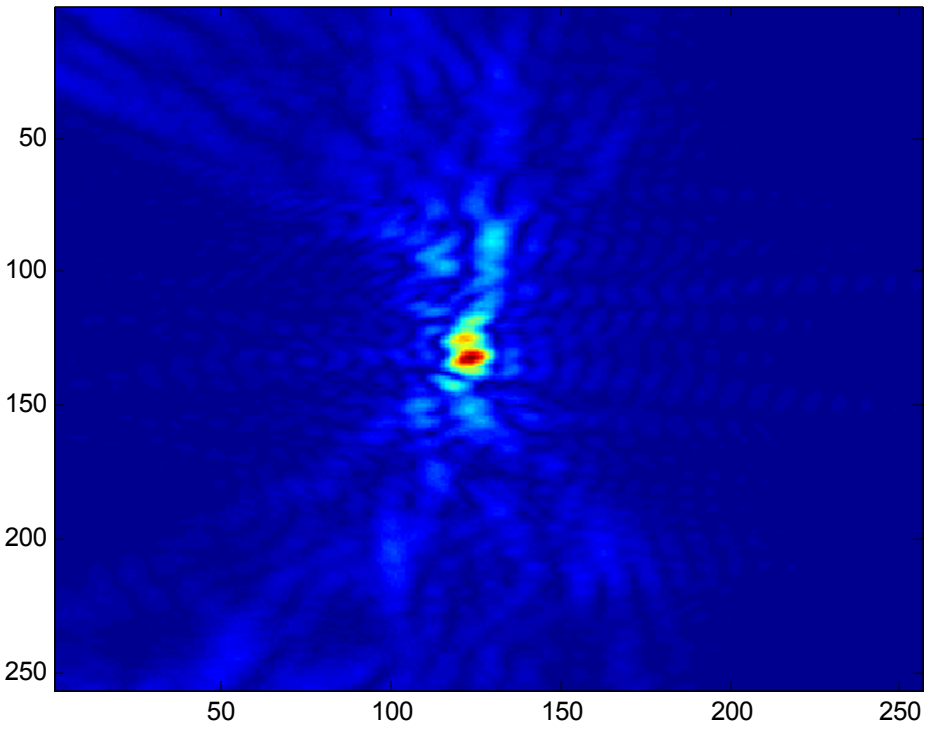


Figure 18: SAR image after pulse compression for spotlight mode with 71 aperture positions.

## 2.2 Strip map Mode for Linear Aperture

### *2.2.1 With 71 aperture points*

RAW data matrix of the stripmap mode is represented in Fig.19 which does not look like a perfect curve unlike spotlight mode. This is because in the stripmap mode the antenna does not always receive stronger reflections from the target reflector at all the aperture positions. In Fig.19 the plot shows range samples on *x*-axis and aperture position on *y*-axis, from the figure it is observed that in strip map mode stronger reflections are received from the aperture points in the middle and weaker reflections are received from the farther aperture points.

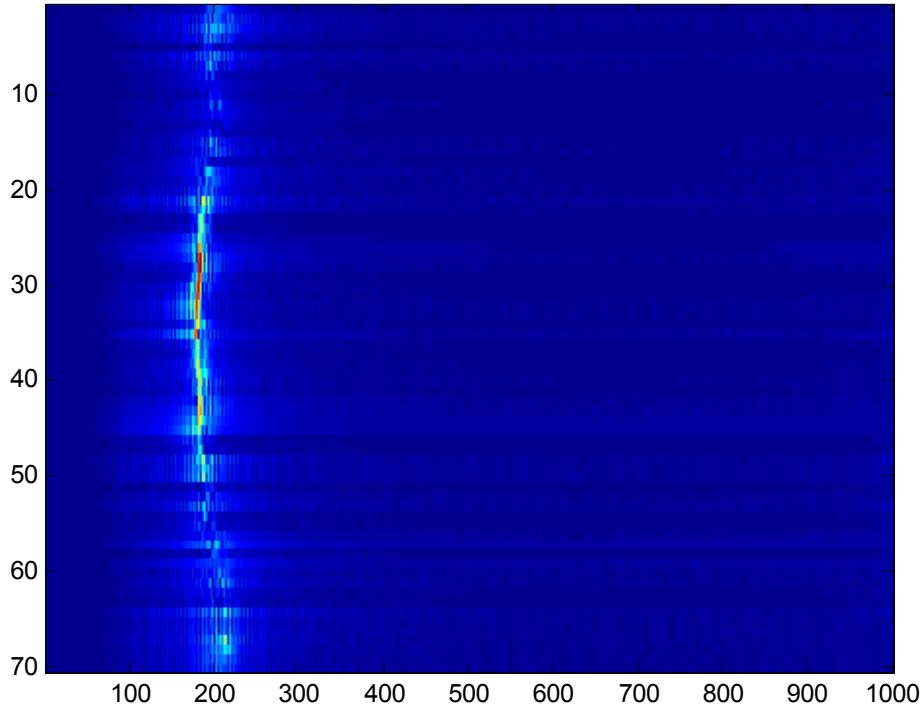


Figure 19: SAR raw data matrix for stripmap mode

SAR image for the stripmap mode without pulse compression can be seen in Fig.20. It can be observed that inspite of weaker reflections from few aperture positions SAR image resolution in stripmap mode is almost similar to that of spotlight mode results. However side lobes are not clearly visible. This could degrade the SAR image quality during real time. In this experiment parameters used are same as shown in Tab.2 except the change in mode of operation. For SAR images *x*-axis represents range resolution and *y*-axis represents azimuth resolution as described before and reflected signal is gated with narrow window width.

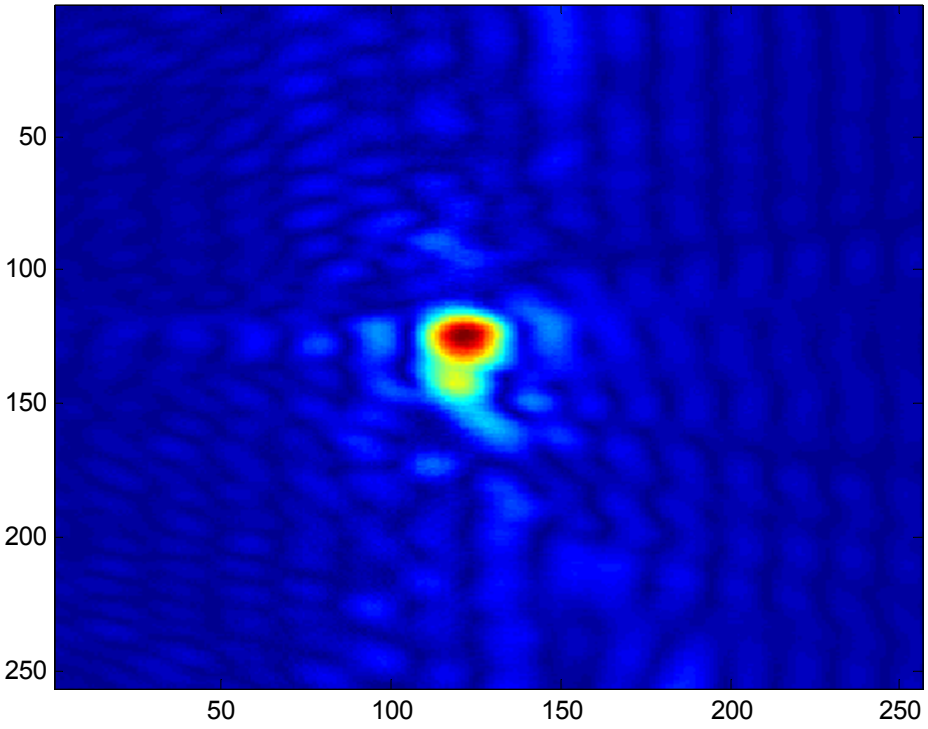


Figure 20: SAR image for stripmap mode without pulse compression

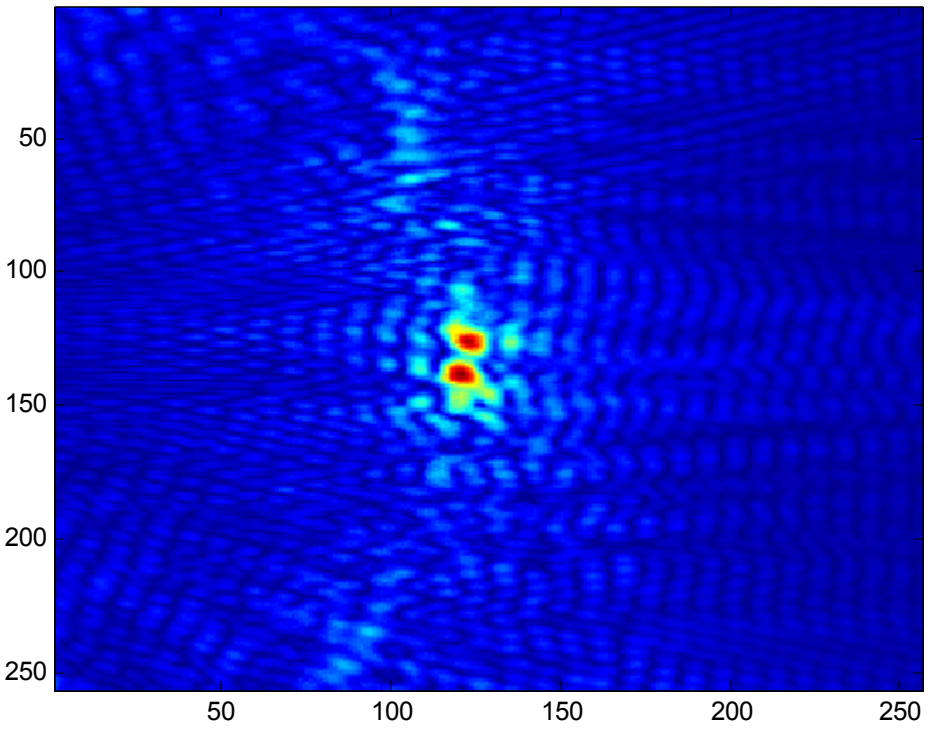


Figure 21: SAR image for stripmap mode with pulse compression without phase correction.

SAR image for stripmap mode after pulse compression is represented in Fig.21. Result shows the SAR image affected by the phase distortion. This result is obtain when the peak corresponding to the corner reflector alone is gated with the window of very less span such that only the reflection corresponding to the target is taken into consideration. After correcting the phase distortion mirror image of the target disappears and a single target could be observed as shown in Fig.22. However these two results are obtained after pulse compression with interpolation at the up sampling rate of 10. Fig.20 shows the result without pulse compression and everything else remaining same. From this particular experiment it was observed that for non pulse compressed result, image was not affected with phase distortions and the shown result is same before or after applying phase correction.

On comparing the results obtained from spotlight mode in Fig.18 and stripmap mode in Fig.22 degradation in the quality of the SAR image is observed in stripmap mode. However the resolutions remain almost the same but the degradation of SAR image quality can cause adverse effects in real time.

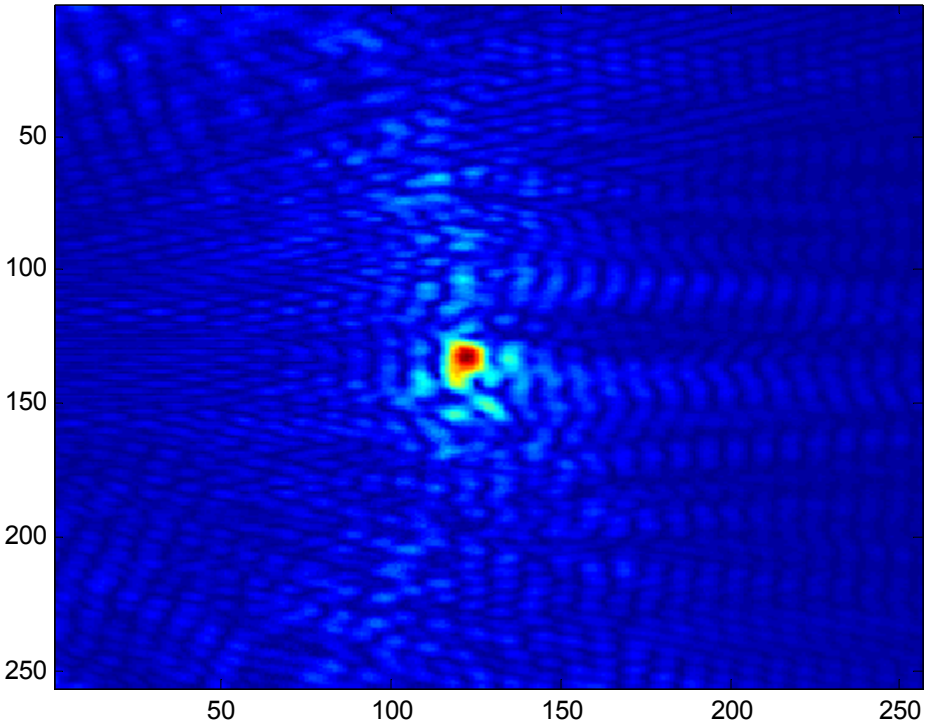


Figure 22: SAR image for stripmap mode with pulse compression after phase correction.

## 2.3 Effects of Gating with wide Window width

### *2.3.1 Strip map Mode for Linear Aperture with 71 aperture points*

In this experiment reflected signal is gated with a wide window width thereby adding the region around corner reflector into consideration. While gating with the wide window width, it is obvious that the reflections are also obtained from other apparatus available in the distance concerning the window width. Thus all these reflections sum up and get mixed into the reflected signal. This causes complete degradation in the SAR raw data as well as the SAR image. This effect is more in strip map mode because of the lack of stronger reflections at the farther end aperture positions. This effect can be observed in the Fig.23 where the reflections corresponding to the corner reflector is buried in the reflections of other apparatus. However from keen observation the curve that corresponds to SAR raw data can be observed. Similar to other SAR raw data results Fig.23 shows range samples on *x*-axis and aperture position on *y*-axis. Parameters used for the experiment are shown in Tab.2.

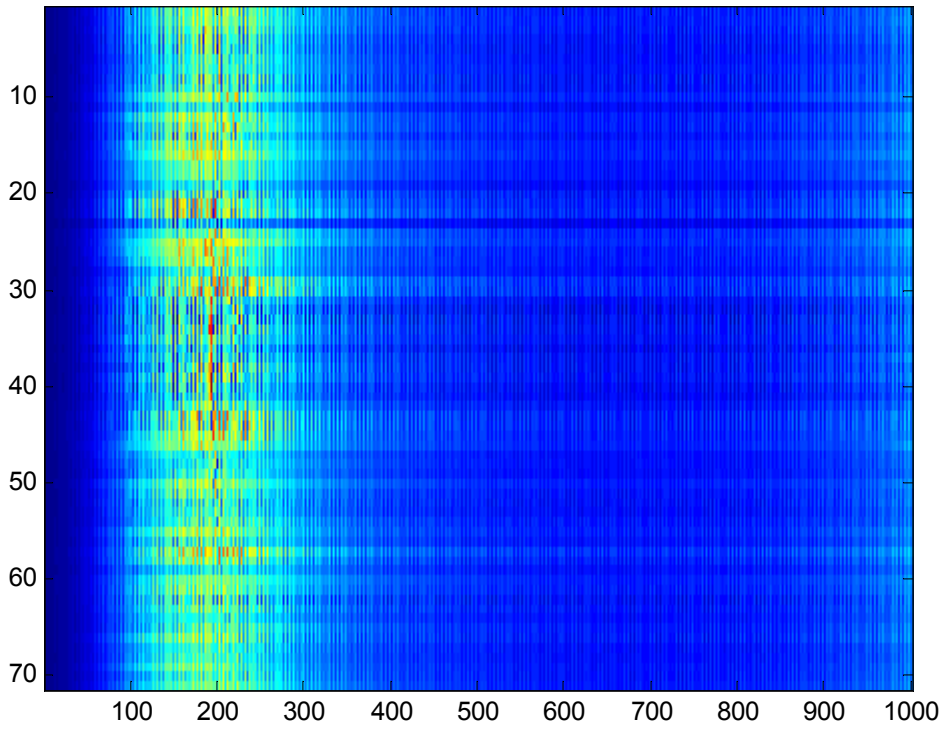


Figure 23: SAR raw data for stripmap mode with wide gating width.

SAR image for stripmap mode with wide gating width is shown in Fig.24 in which complete degradation in the quality of image is observed.

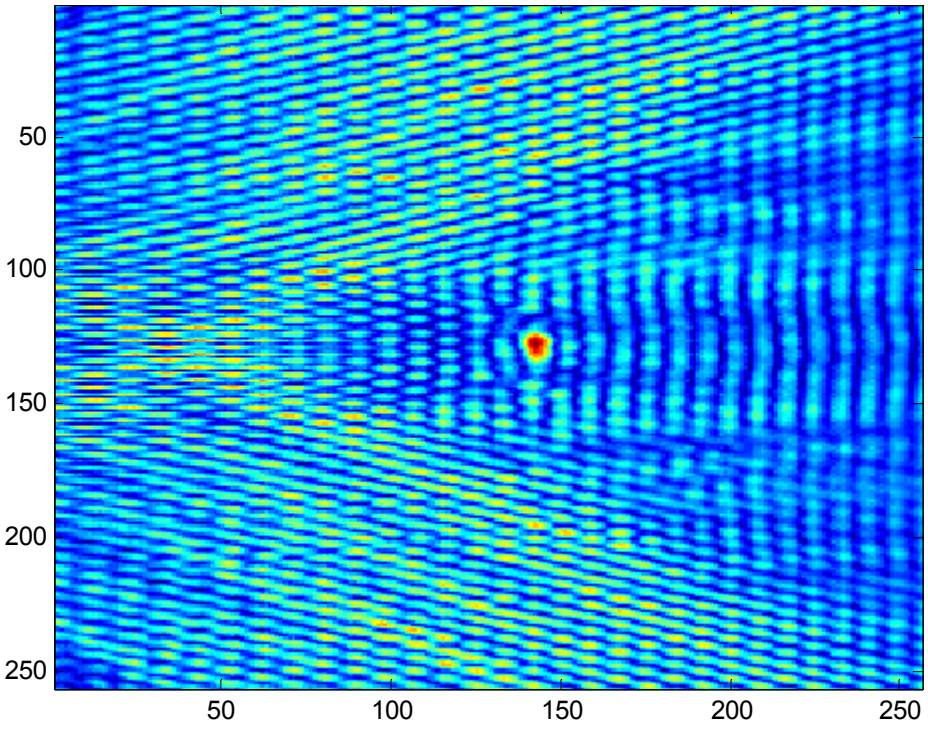


Figure 24: SAR image for stripmap mode with wide gating width.

### 2.3.2 Spotlight Mode for Linear Aperture with 71 aperture points

While dealing with the wide window widths for gating the reflected signal, SAR image is degraded as shown. By observing the results shown in Fig.24 and Fig.26 this degradation is almost similar for spotlight mode and strip map mode but with a slight difference because in spotlight mode we get stronger reflections at all the aperture positions. The difference can be seen only by careful and keen observation. SAR raw data for spotlight mode with wide gating width is shown in Fig.25 and SAR image is shown in Fig.26.

By proper motion error compensation or autofocus correction the quality of such SAR images can be highly enhanced. However in real time it is not possible for the SAR system to focus only on a particular target because the swath area of SAR system corresponds to several kilometres. Thus in real time reflected signal is gated only with wide window widths and to get better quality of the SAR image autofocus correction can be the solution. The results obtained after autofocus correction can be seen in [1] and [2].

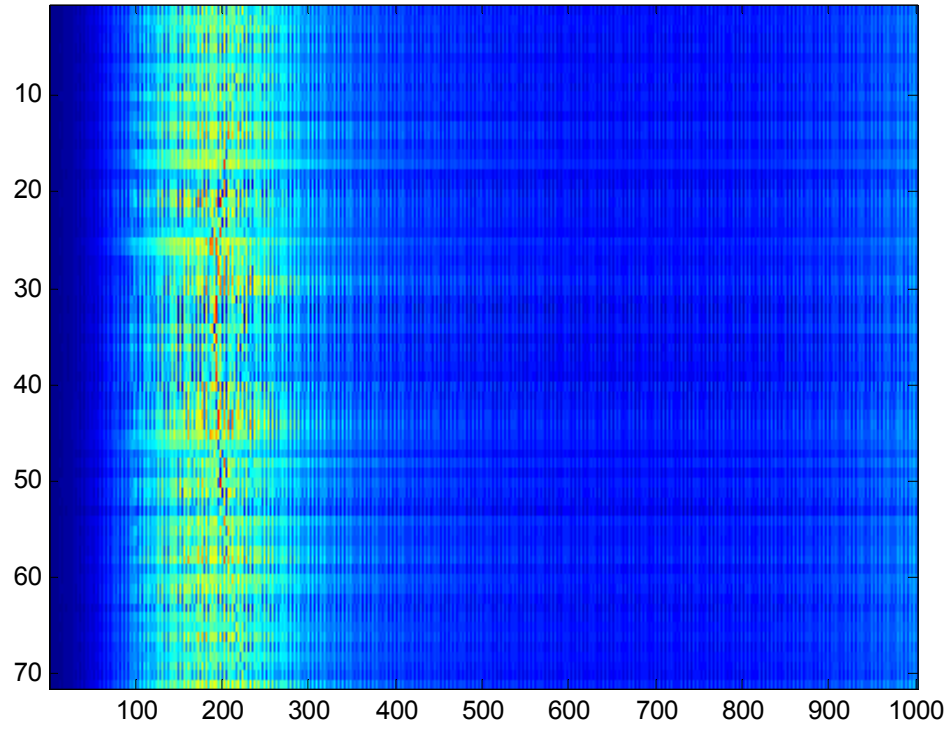


Figure 25: SAR raw data for spotlight mode with wide gating width.

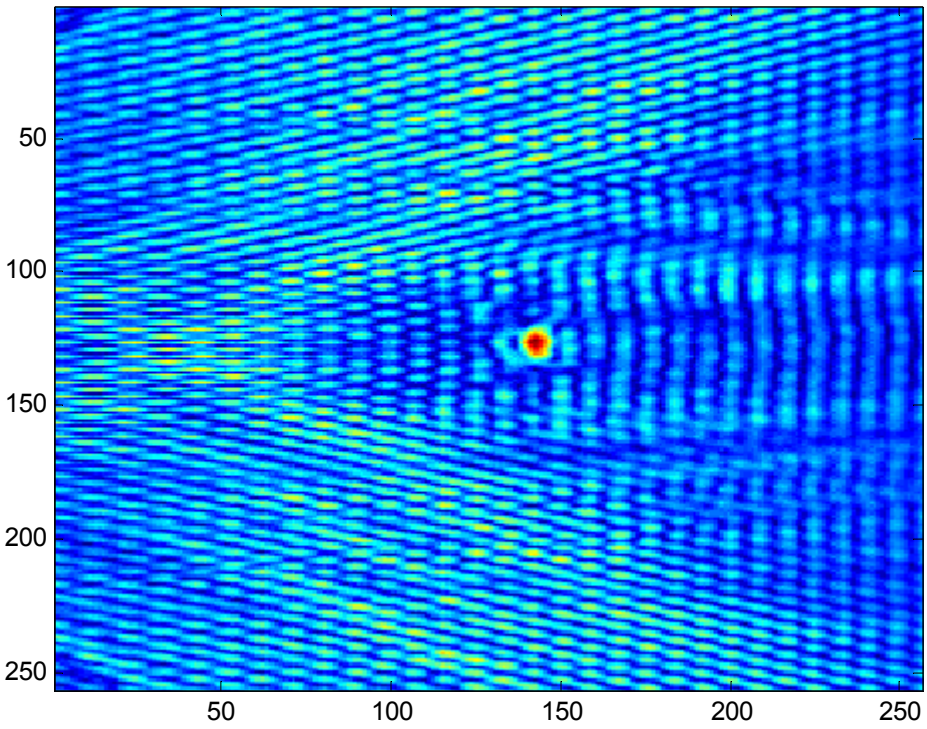


Figure 26: SAR image for spotlight mode with wide gating width

## 2.4 Effects of the No. of Aperture Positions

From the Fig.27 effects of having high and low aperture positions is observed. By looking at the figure the necessity of acceptable aperture step can be observed. With the parameters used in Tab.2 and according to the condition for aperture step derived in [1], 71 is the number of acceptable aperture positions. In this figure SAR image is obtained for different number of aperture positions and it could be observed that for 68 aperture positions the result is very clear and saturated. This means that even if we further increase the number of aperture positions the result is still the same since it has achieved its highest quality level. Apart from the quality orthogonal side lobes and non orthogonal side lobes are perfectly visible on following the derived expression.

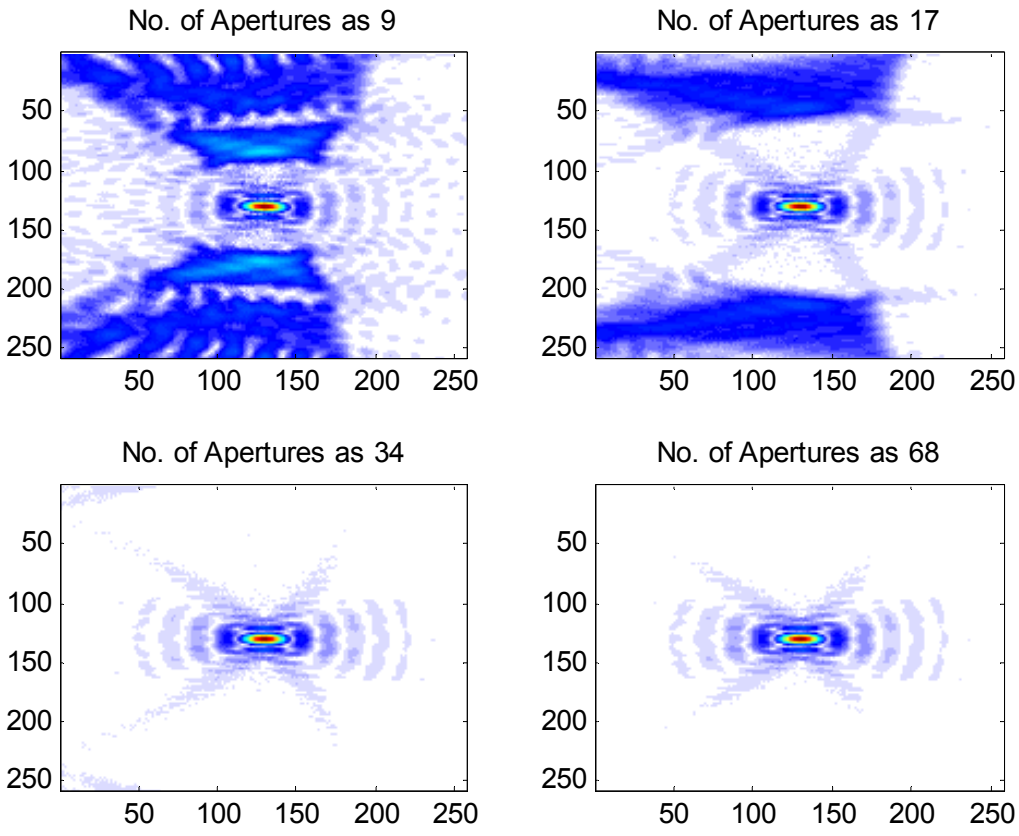


Figure 27: Effects of the number of aperture positions.

From the results represented in Fig.27 the expression derived in [1] is validated and to obtain a better quality SAR image acceptable number of aperture positions and aperture step should be considered.

## 2.5 Effects of Integration angle

This experiment focuses on observing the impact of integration angle on the SAR image resolution particularly the azimuth resolution. Parameters used in this experiment are shown in Tab.3.

| Parameter | Setting |
|---|---|
| The highest processing frequency | 2.5 GHz |
| The lowest processing frequency | 1.5 GHz |
| Altitude of the ground-based SAR system | 1.25 m |
| Minimum range | 2.86 m |
| Aperture step | 0.05 m |
| Number of aperture positions | 11 |
| Synthetic aperture length | 0.55 m |
| Integration angle | $10^0$ |

Table 3: Parameter for experimentation with low integration angle

The SAR image obtained for system with low integration angle and acceptable no of aperture positions and aperture step as derived in [1], can be seen in Fig.28. Mode of operation is strip map mode and wide window width (width is less when compared to section 2.3) is considered for reflected signal gating because of which unwanted reflections can be observed. Comparing this image from various other results of linear aperture it can be observed that, the SAR image in Fig.28 shows much decrease in azimuth resolution (on *y*-axis) and constant range resolution (on *x*-axis). This is because of the fact that azimuth resolution depends on the angle of integration and is directly proportional to it. As the integration angle increases the azimuth resolution also increases. It is to be noted that the SAR images in this section corresponds to pulse compressed results.

The SAR image obtained for the parameters used in Tab.3 and the mode of operation as stripmap mode but with narrow reflected signal gating width is shown in Fig.29. By considering narrow gating window width unwanted reflections are avoided and good quality of SAR image is maintained. For simplicity in signal processing to get good quality SAR image it is better to consider narrow gating width, which prevents complexity of autofocussing needed when wide gating width is considered. However it should be remembered that in real time wide gating width is considered.

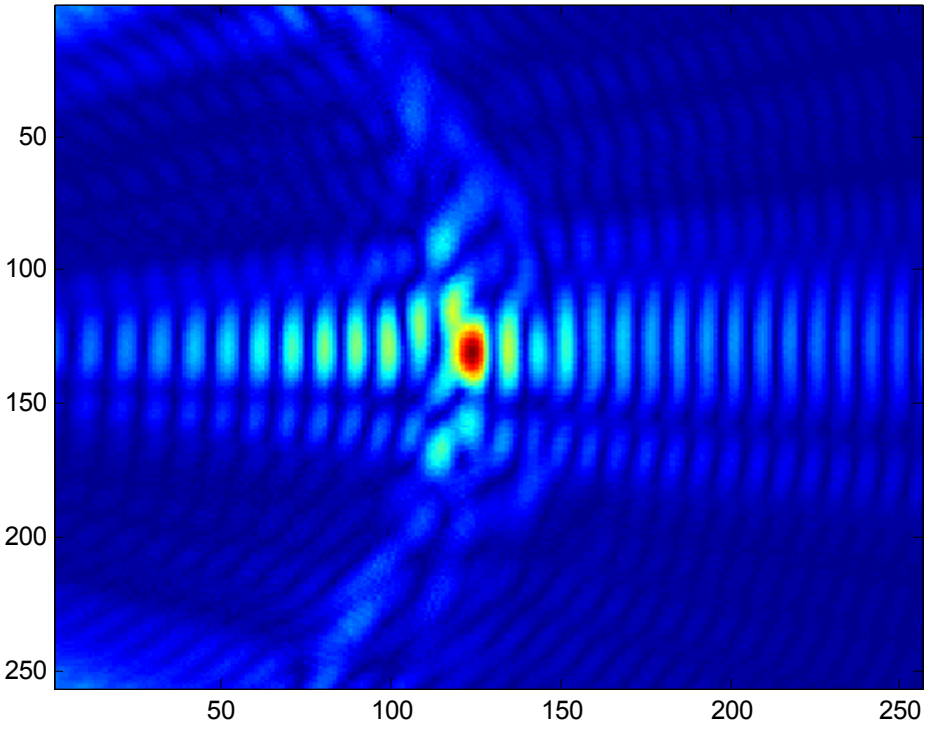


Figure 28: Effects of Integration angle on SAR image with wide gating width.

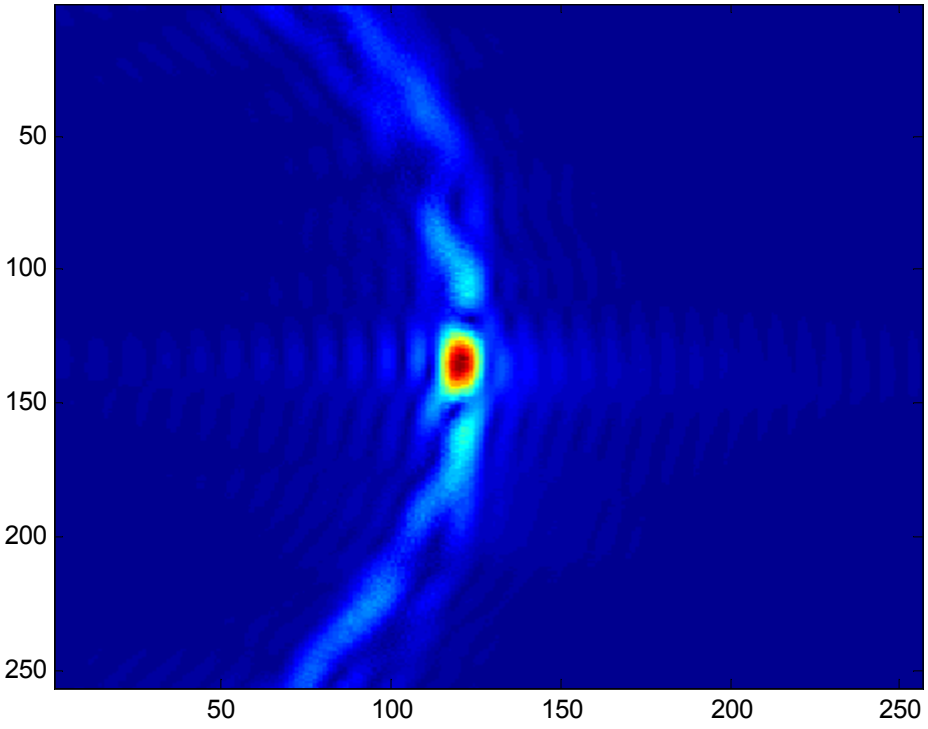


Figure 29: Effects of Integration angle on SAR image with narrow gating width.

## 2.6 Circular Aperture with 32 aperture points

For circular aperture only spotlight mode can be used since the circular path makes even stripmap mode act as spotlight. Parameters used in this section are shown in Tab.4. SAR image without pulse compression for circular aperture with 32 aperture positions representing a semicircle is shown in Fig.30. Circular aperture can be seen in Fig. 5 & Fig.6.

| Parameter | Setting |
|---|---|
| The highest processing frequency | 2.5 GHz |
| The lowest processing frequency | 1.5 GHz |
| Altitude of the ground-based SAR system | 1.25 m |
| Constant range | 2.86 m |
| Aperture step | 0.24 m |
| Number of aperture positions | 32 |
| Synthetic aperture length | 7.70 m |
| Integration angle | $180^0$ |

Table 4: Parameter for experimentation with circular aperture

It should be understood that in circular aperture azimuth direction is not present and thus azimuth resolution does not exist. Only one resolution is available and is termed as spatial resolution. By comparing the results corresponding to linear aperture and circular aperture, enhancement of resolution in circular aperture as stated in [2] can be observed.

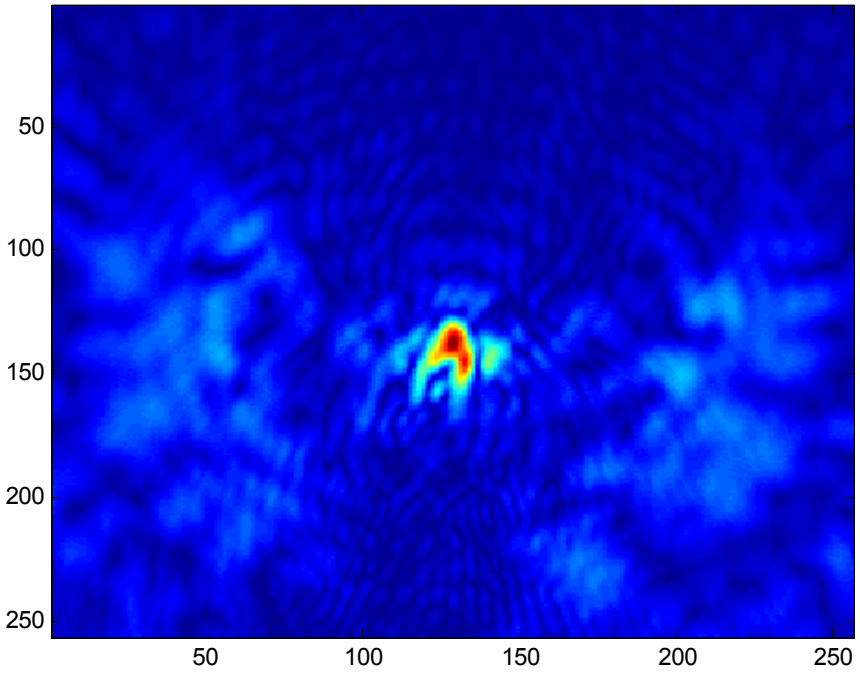


Figure 30: SAR image without pulse compression for 32 apertures.

SAR image after pulse compression for circular aperture with 32 aperture positions representing a semicircle is shown in Fig.31.

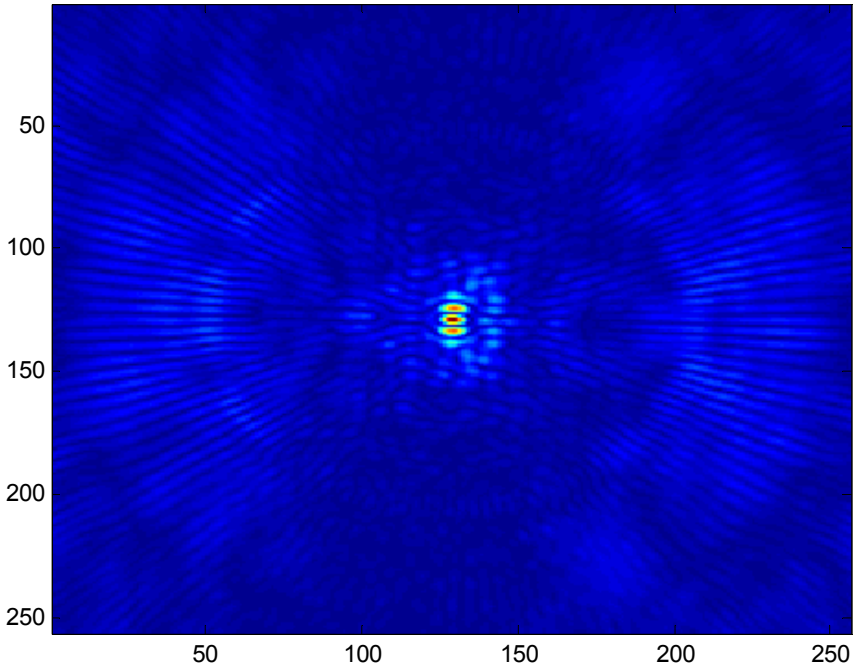


Figure 31: SAR image after pulse compression for 32 apertures

## 2.7 Experiment with the moving target

When the target is moving at the speed of $1/10^{th}$ of the velocity of SAR platform, the result is obtained as a curve as shown in the Fig.32. CARABAS system parameters are used.

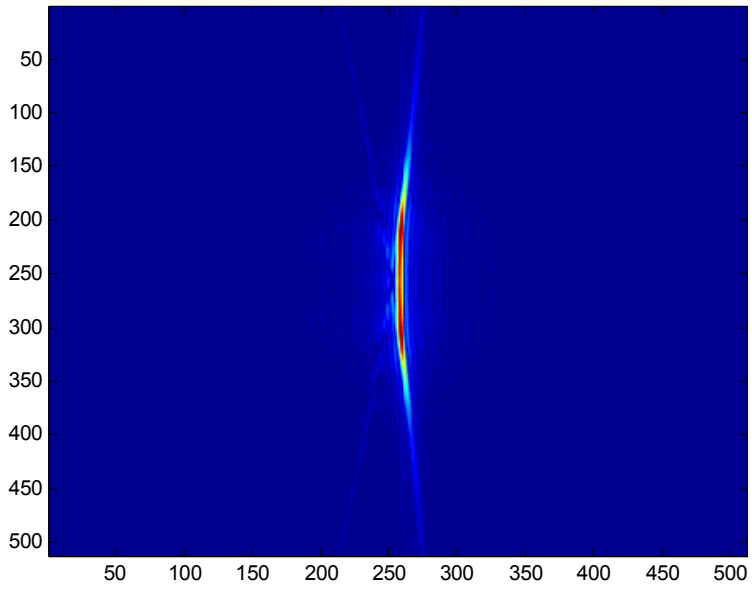


Figure 32: SAR image for moving target with velocity $1/10^{th}$ of SAR platform.

When the target is moving at the speed of $1/5^{th}$ of the velocity of SAR platform, the result is obtained as a long curve as shown in Fig.33. This means that the length of the SAR image curve depends on the relative velocity of the target with respect to the velocity of the SAR platform. On comparing Fig.32 & 33 the SAR image curve is long when the relative velocity is less, curve is short when relative velocity is more.

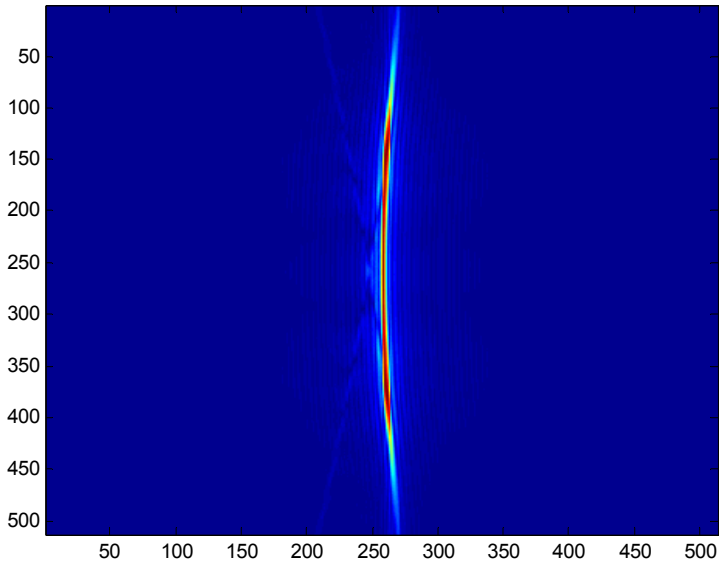


Figure 33: SAR image for moving target with velocity $1/5^{th}$ of SAR platform.

# References

[1] Viet T. Vu, Dheeraj N. Nehru, Thomas K. Sjögren and Mats I. Pettersson, "An experimental ground-based SAR system for studying SAR fundamentals", in *Proc. APSAR 2013*, Tsukuba, Japan, Sep. 2013, accepted for publication.

[2] Dheeraj N. Nehru, Viet T. Vu, Thomas K. Sjögren and Mats I. Pettersson, "SAR resolution enhancement with circular aperture in theory and empirical scenario", in Proc. IEEE RadarCon 2014, Cincinnati, USA, May 2014, submitted for publication.